Title

Critical test of the assumption that the hypothalamic entopeduncular nucleus of rodents is homologous with the primate internal pallidum.

Journal

The Journal of Comparative Neurology, 531(16)

Authors

Puelles, Luis
Stühmer, Thorsten
Rubenstein, John
et al.

Publication Date

2023-11-01

DOI

10.1002/cne.25536

Peer reviewed

HHS Public Access

Author manuscript

J Comp Neurol. Author manuscript; available in PMC 2024 November 01.

Published in final edited form as:

J Comp Neurol. 2023 November ; 531(16): 1715–1750. doi:10.1002/cne.25536.

Critical test of the assumption that the hypothalamic entopeduncular nucleus of rodents is homologous with the primate internal pallidum

Luis Puelles[1], **Thorsten Stühmer**[2,‡], **John L. R. Rubenstein**[2], **Carmen Diaz**[3]

[1]Department of Human Anatomy and Psychobiology and IMIB-Arrixaca Institute, University of Murcia, El Palmar (Murcia), 30120, Spain

[2]Nina Ireland Laboratory of Developmental Neurobiology, Department of Psychiatry, UCSF Medical School, San Francisco, California.

[3]School of Medicine and Institute for Research in Neurological Disabilities, University of Castilla-La Mancha, Albacete, 02006, Spain.

Abstract

The globus pallidus of primates is divided conventionally into distinct internal and external parts. The literature repeats since 1930 the opinion that the homolog of the primate internal pallidum in rodents is the hypothalamic entopeduncular nucleus (embedded within fiber tracts of the cerebral peduncle). To test this idea, we explored its historic fundaments, checked the development and genoarchitecture of mouse entopeduncular and pallidal neurons, and examined relevant comparative connectivity data.

We found that the extratelencephalic mouse entopeduncular structure consists of four different components arrayed along a dorsoventral sequence in the alar hypothalamus. The ventral entopeduncular nucleus (EPV), with GABAergic neurons expressing *Dlx5&6* and *Nkx2-1*, lies within the hypothalamic peduncular subparaventricular area. Three other formations, the dorsal entopeduncular nucleus (EPD), the prereticular entopeduncular nucleus (EP_{PRt}) and the preeminential entopeduncular nucleus (EP_{PEm}) lie within the overlying paraventricular area, under the subpallium. EPD contains glutamatergic neurons expressing *Tbr1, Otp*, and *Pax6*. The EP_{PRt} has GABAergic cells expressing *Isl1* and *Meis2*, whereas the EP_{PEm} population expresses *Foxg1* and may be glutamatergic. Genoarchitectonic observations on relevant areas of the mouse pallidal/diagonal subpallium suggest that the globus pallidus of rodents is constituted as in primates by two adjacent but molecularly and hodologically differentiable telencephalic portions (both expressing *Foxg1*). These and other reported data oppose the notion that the rodent extratelencephalic entopeduncular nucleus is homologous to the primate internal pallidum. We suggest instead that all mammals, including primates, have dual subpallial globus pallidus components and also a comparable set of hypothalamic entopeduncular nuclei. Remarkably, there is close similarity in

Correspondence: Luis Puelles (puelles@um.es) and Carmen Diaz (carmen.diaz@uclm.es).
‡Present address: Comprehensive Cancer Center Mainfranken, University Hospital Würzburg, 97080, Würzburg, Germany.

Conflict of Interest

The authors declare that the research was conducted in the absence of any commercial or financial relationships that could be construed as a potential conflict of interest.

some gene expression properties of the telencephalic internal globus pallidus and the hypothalamic EPV. This apparently underlies their notable functional analogy, sharing GABAergic neurons and thalamopetal connectivity .

Graphical Abstract

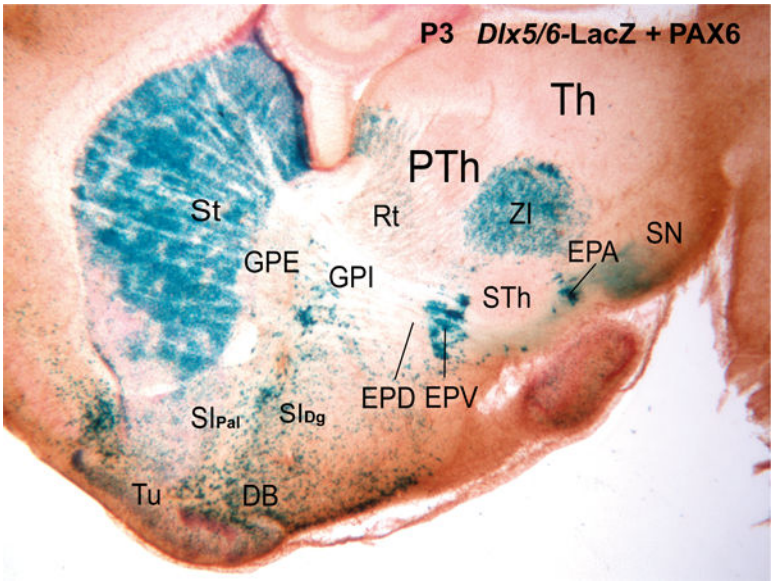

Various molecular and hodological data illustrate external and internal parts of the mouse globus pallidus, comparable to those in primates, whereas the distant hypothalamic entopeduncular population shows independent dorsal and ventral parts. The conventional hypothesis that the rodent entopeduncular nucleus is homologous to the primate internal pallidus is therefore inconsistent.

Keywords

entopeduncular nuclei; internal globus pallidus; hypothalamus; basal ganglia; homology; motor network

1. INTRODUCTION

The current standard concept of the pallido-entopeduncular complex of rodents compares it as a whole to the primate globus pallidus, which is clearly composed of distinct external and internal globus pallidus parts (e.g., Dudman & Gerfen, 2015; Graybiel, 1984; Heimer et al., 1991, 1995; Nieuwenhuys et al., 2008; Percheron et al., 1994). It is assumed by most experts in the field that the rodent *globus pallidus* (found within the telencephalon just medial to the striatal putamen) is strictly homologous only with the external pallidal segment of primates, whereas a separate *entopeduncular nucleus* (found interstitial to the hypothalamic course of the cerebral peduncle, close to the subthalamic nucleus) is held to be homologous with the internal pallidal segment of primates (e.g., Dudman & Gerfen, 2015). However, Paxinos and Watson (2014; their Figs.43–46) exceptionally distinguish external and internal

globus pallidus components within the rodent telencephalic pallidum, admitting that the mouse entopeduncular nucleus is strictly a non-pallidal hypothalamic structure as argued by Puelles et al. (2012, 2013). A recent transcriptomic analysis of mouse entopeduncular neurons and their connections (Wallace et al., 2017), as well as a review of the evolution of basal ganglia in mammals and other vertebrates (Reiner, 2016), followed the traditional homology assumption in spite of presenting contrary hodological and comparative evidence, respectively, no doubt influenced by the accumulated authority of the widespread literature opinions.

The traditional entopeduncular/inner globus pallidus homology concept needs re-evaluation because it has not been corroborated by comparative neuroanatomy (e.g., Medina, 2007, 2009; Medina & Abellán, 2012; Medina et al., 2005, 2014; Reiner, 2007; Reiner et al., 1998, 2004, 2005; Stephenson-Jones et al., 2011, 2012), and because there is consensus in this scientific field that the main details of forebrain structure of *all* mammals coincide in relative topological positions, genetic background, and developmental origin (reviews in Heimer et al., 1995; Medina & Abellán, 2012; Medina et al., 2014; Paxinos & Watson, 2014; Siskos et al., 2021; Striedter & Northcutt, 2020; Swanson, 2003). Our analysis explores the historic background out of which this confusing comparative opinion seems to have arisen, and then critically examines the scenario in the light of modern genoarchitectural data and some hodological data. This endeavor drives us to the conclusion that a concatenation of historic misconceptions, imprecise embryology, and the existence of some remarkably convergent molecular and hodological similarities led to the present pallido-entopeduncular homology myth.

In a first approximation to the topic, it can be appreciated that modern arguments adduced to support pallido/entopeduncular homology in rodents concentrate on the existence of *similar connections* (e.g., Dudman & Gerfen, 2015). However, similarity of connections can be duplicated convergently under particular conditions of phenotypic parallelism arising at different locations of the forebrain Bauplan, without justifying a homology proposal. This case should be interpreted as an analogy (*functional similarity* of different structures) rather than as a homology. Indeed, mere similarity of neural connections, without complementary evidence of a topologically and causally comparable developmental origin of the neurons compared does not establish proof for homology *per se* (Medina, 2007; Nieuwenhuys & Puelles 2016; Puelles, 2022; Puelles & Medina, 2002). Taken together with other recent molecular and experimental data, our results question the present developmental and anatomic scenario sketched due to lack of a solid underpinning for the postulated pallido/entopeduncular homology between rodents and primates.

1.1 Historic antecedents of the pallido/entopeduncular homology notion.

Spatz (1921, 1922, 1924, 1925) apparently originated 100 years ago the notion about a developmental relationship of some hypothalamic primordia with pallidal telencephalic formations in adult primates and man. He mapped metallic iron in this area using Perl's histochemical reaction and noted shared high iron content in the human subthalamic and pallidal nuclei. In the context of Herrick's columnar model of the diencephalon and hypothalamus (Herrick, 1910), this finding led Spatz to postulate a common developmental

origin of these iron-rich elements in the 'diencephalon', specifically in a "dorsal longitudinal zone of its ventral column, the hypothalamus", also known as "subthalamus"[1]. One aspect of histochemical similarity within a then hypothetical subthalamo-strio-pallidal functional system (the modern idea of 'basal ganglia' was still distant) was thus hypothesized to reveal a *common hypothalamic origin* of the *whole pallido-subthalamic complex*. Nobody defends this notion now. Note that, according to Spatz's conception, the telencephalic ganglionic eminences only would produce striatal tissue, a viewpoint shared by various authors at that time (see the same idea, e.g., in Ganser, 1882; and His, 1893a,b; 1904). This is now negated by substantial genoarchitectonic and, particularly, mutation analysis, plus fate mapping data (Flames et al., 2007; Flandin et al., 2010; Kimura et al., 1996; Marín et al., 2002; Sussel et al., 1999). Spatz's columnar "dorsal *longitudinal* zone of the hypothalamus" does reach the subpallium at the telencephalic stalk, and strictly corresponds to the *transverse* hp1 prosomere, a hypothalamo-telencephalic domain, whose hypothalamic subregion was renamed 'peduncular hypothalamus' within the prosomeric model (Puelles et al., 2012; Puelles & Rubenstein, 2015).

It was further conjectured by Spatz and various later authors studying basal mammalian (including rodent), human and monkey embryos that during forebrain morphogenesis there occurs either tangential migration or morphogenetic displacement of the *originally hypothalamic* pallidal primordia into the telencephalon (Kuhlenbeck, 1924, 1927, 1954, 1973; Kuhlenbeck & Haymaker, 1949; Spatz, 1921, 1922, 1924, 1925; also, Spatz's pupil Richter, 1965 and Kuhlenbeck's collaborator Christ, 1968[2]). The hypothetic full developmental process was described in primate embryos (Richter, 1965). It was thought that basal mammals (including rodents) showed a first partial evolutionary step in, in which only the external globus pallidus

Recently the study of Silberberg et al. (2016; their Fig. 2) ascribed the primary origin of the mouse external pallidum to the *pallidal* or dorsal subpallial sector of the medial ganglionic eminence (Pal), whereas the internal pallidum was postulated to arise from the adjacent *diagonal* (Dg) subpallial sector of the MGE, found caudomedially within this eminence (we previously called it the 'anterior entopeduncular domain' -AEP- a classic name with various semantic problems causing the change to 'diagonal domain or area' proposed by Puelles in 2011 in the mouse brain ontology associated to the Allen Developing Mouse Brain Atlas, as well as in Puelles et al., 2013). Some gene markers characterizing differentially the subpallial pallidal and/or diagonal domains of the MGE become first expressed at E9.5-E10 in the mouse, well before any tangential migration from the hypothalamus can occur (e.g., Puelles et al., 2016).

This analysis applies equally to other mammals and tetrapods in general (birds; reptiles; amphibia; Reiner, 2016; Reiner et al., 1998, 2004, 2005), as well as to gnathostome fishes,

[1]These names are columnar terms, implying the modernly contradicted assumption that the forebrain axis ends in the telencephalon, so that subthalamus and hypothalamus would lie "ventral" to thalamus; see discussion in Puelles et al. (2012); the reformulated definition of the forebrain length axis proposed in the modern prosomeric model returns roughly to the pioneering axial concept of His (1893a,b), though using molecularly characterized longitudinal landmarks (e.g., the roof plate, the forebrain alar-basal boundary, the floor plate, and the underlying notochord; Puelles, 2018; Puelles & Rubenstein, 2015; Puelles et al., 2012).

[2]Note the theoretic part of Christ's publication was written by Kuhlenbeck, as is indicated in a footnote in the first page.

where a molecularly comparable primarily telencephalic pallidal anlage exists, even in cases where a ventricular bulge of the pallidal progenitor domain is absent (Cobos et al., 2001a,b; Marin et al., 1997; Medina et al., 2014; Métin et al., 2007; Moreno et al., 2008a,b,c, 2010, 2018; Puelles et al., 2000; Smeets et al., 2000). Recently, agnathans are thought to have also a telencephalic pallidal primordium and correlative pallido-pallial migrations (Villar-Cervino et al., 2008; Pombal et al., 2009; Martínez-de-la-Torre et al., 2011; Stephenson-Jones et al., 2011, 2012; Grillner & Robertson, 2016; Sugahara et al., 2022).

It may be concluded accordingly that modern descriptive, autoradiographic, and molecular studies of developing rodents have confirmed that the hypothalamic entopeduncular and subthalamic nuclei develop and stay separately within the peduncular hypothalamus, whereas dual pallidal primordia develop within the pallidal and diagonal subareas of the medial ganglionic eminence of the telencephalon. We therefore deduce that primates and humans would be expected to have comparable hypothalamic entopeduncular cell populations, besides their bipartite globus pallidus and the well-known subthalamic nucleus.

The conventional pallido/entopeduncular homology hypothesis between the rodent and primate internal pallidal portion is accordingly contradicted by diverse lines of evidence.

Such long-standing contradictory data are being ignored by the experts that write the chapters on ‘Basal ganglia’ in important treatises or specialized books, possibly due to a centering of their attention upon apparent *similarities in connectivity patterns* (e.g., Heimer et al., 1995; Alheid et al., 1990; Gerfen, 2004; an exception is found in Medina, 2007; Martinez-Garcia et al., 2007, and Medina & Abellán, 2012, as well as in Puelles et al., 2013, and Paxinos & Watson, 2014). Although the classic conjecture of a diencephalic or hypothalamic pallidal origin probably persists more by force of tradition than of conviction, alternative modern developmental underpinnings of the entopeduncular/pallidal homology assumption have not been advanced so far. How should the existing data be interpreted? Answering this question is our main goal, for which we will examine postnatal and embryonic genoarchitectonic material identifying the characteristic molecular profiles of the relevant cell populations and their respective histogenetic origins. Complementary observations illustrate some important hodological properties.

2. MATERIALS AND METHODS

2.1 Animals

All experimental procedures with transgenic mice (see below) were approved by the Committee on Animal Research at University of California, San Francisco (CA), and mouse colonies maintained in accordance with National Institutes of Health and UCSF guidelines. Mouse brain material from diverse embryonic and postnatal stages was examined in sagittal, horizontal, and coronal section planes. Additionally, we analyzed *in situ* hybridization (ISH) images downloaded from the Allen Developing Mouse Brain Atlas (https://developingmouse.brain-map.org) and Allen Mouse Brain Atlas (https://mouse.brain-map.org/). In this case our analysis was focused on embryonic (E) stages (E11.5, E12.5, E13.5, E15.5, E18.5) and postnatal P1 stage in sagittal sections (and coronal ones when

available; no horizontal sections are offered in this database). According to documentation given by the Allen platform, male specimens of the C57BL/6J mouse strain were used for the E15.5 through adult stages. We have also analyzed data from the Allen Mouse Brain Atlas Mouse Brain Connectivity available at: https://connectivity.brain-map.org).

2.2 Transgenic animals

The isolation of zebrafish *dlx4/6* forebrain enhancer elements, construction of the *zfdlx4/6*LacZ transgenic vector, and the characterization of *LacZ* expression (encoding β-galactosidase) using the X-gal histochemical reaction in transgenic mice (strain C57BL/6) with respect to that of the endogenous *Dlx5* and *Dlx6* genes, are described in Zerucha et al. (2000) and Stühmer et al. (2002a,b). The propagation of the transgene appears to be stable, as no change in the pattern or intensity of beta-galactosidase expression has been noted for many generations.

2.3 Preparation of tissue

We studied mouse brains at embryonic [E] ages E11.5, E12.5, E13.5, E14.5, E15.5, E16.5, and postnatal [P] ages P0, P3, P20, and P56. For the preparation of embryonic brain tissue, timed pregnant dams were killed by cervical dislocation, embryos removed, and the brains dissected in cold phosphate-buffered saline (PBS: 137 mM NaCl, 2.7 mM KCl, 1.8 mM KH2PO4, 5.1 mM Na2HPO4, pH 7.4). The tissue was fixed in cold 4% paraformaldehyde/PBS between 30 min (E11.5) and 2 h (E17.5). For the preparation of postnatal tissue, animals were anaesthetized with 2% chloral hydrate/PBS, and perfused intracardially with 10 ml (at P0) up to 50 ml (at P13 and older) cold 4% paraformaldehyde/PBS (occasionally also with 0.15% glutaraldehyde). Following dissection, postnatal brains were postfixed in the same solution for 3 hours. All tissue was rinsed overnight in PBS and either sectioned directly or stored at −20°C in a solution of 30% v/v ethylene glycol, 30% v/v glycerol, 40% v/v PBS. Brains stored in this way were rinsed overnight in PBS prior to sectioning.

2.4 Sectioning of tissue

Except for very early ages (E11.5 to E13.5), the brains were halved along the midline to obtain transverse or coronal and sagittal (or horizontal) sections from the same specimen. Embryonic brains were embedded in 5% low melting point agarose to increase the stability and ease of handling of the sections. Agarose blocks tailored to provide standard coronal, sagittal or horizontal planes of section were habitually prepared. Occasionally additional blocks were aimed to obtain sections strictly transverse or horizontal to the prosomeric length axis (i.e., ending rostrally in the hypothalamus; Puelles et al., 2012). For sectioning, the tissue blocks were mounted, immersed in PBS and cut into series of 100 μm-thick slices with a vibrating blade microtome (Leica). Sections were immediately used for the X-gal staining reaction.

2.5 X-gal (5-bromo-4-chloro-3-indolyl-β-D-galactopyranoside) staining

Sections were immersed in a solution of 10 mM TrisHCl (pH 7.3), 0.005% sodiumdesoxycholate, 0.01% Nonidet P40, 5 mM K4Fe (CN)6, 5 mM K3Fe(CN)6, 2

mM MgCl2, 0.8 mg/ml X-gal (stock solution: 40 mg/ml in dimethylformamide) and incubated overnight at 37°C. The end of the reaction was decided by visual inspection. A non-counterstained series of sections was rinsed in PBS, cleared for 30 min in 50% v/v glycerol in PBS, sequentially mounted on slides, coverslipped, and photographed. Two or three parallel series of sections of each brain were used for immunocytochemistry and counterstaining.

2.6 Immunohistochemistry (IHC)

Our immunohistochemical reaction protocol was described in detail elsewhere (Ferran et al. 2015). The primary antibodies used are described in Table 1. After the X-gal reaction was stopped, sections to be counterstained were thoroughly rinsed in PBS, and blocked with 1% BSA, before applying a primary antibody. Standard biotinylated secondary antibody and avidin-HRP treatments preceded diaminobenzidine visualization of the reaction product and optional weak neutral red counterstaining of the sections.

2.7 Reverse transcriptase-polymerase chain reaction (RT-PCR)

Otp, *Nkx2-1*, and *Pax6* cDNA fragments were obtained by reverse transcription (RT). RNA was individually extracted with Trizol reagent (Invitrogen, Carlsbad, CA, Cat. 10296–028) from freshly dissected brains of *Mus musculus.* The RNA was treated with DNase I (Invitrogen, Cat. 18068–015) for 15 min at room temperature (RT), and the enzyme was then inactivated at 65ºC. Afterwards, RNA samples were converted to single-stranded cDNA with Superscript III reverse transcriptase (Invitrogen, Cat. 18080–044) and oligo-dT-anchored primers. The resulting first-strand cDNA (0.5µl of the reverse transcription reaction) was used as a template for the PCR reaction, which was performed in presence of Taq polymerase (Promega, Cat. M8305) and the gene-specific primers for *Otp*, *Nkx2-1*, and *Pax6* mRNAs.

The PCR conditions used were an initial denaturation step at 94ºC for 5 min, then 35 cycles (30s at 94ºC, plus 1 min at Tm temperature (58ºC), and 1 min at 72C), followed by 20 min at 72ºC. The PCR products were cloned into the pGEM-T Easy Vector (Promega, Cat. A1360), and sequenced (SAI, University of California, San Francisco (CA).

2.8 In situ hybridization (ISH)

The tissues were processed for *in situ* hybridization (ISH) with

digoxigenin-UTP-labeled antisense riboprobes. Sense and antisense digoxigenin-labeled riboprobes for mouse *Otp*, *Nkx2-1*, and *Pax6* were synthesized following the manufacture's recommendations (Roche Diagnostics S.L., Applied Science, Barcelona, Spain), and applying specific polymerases (Fermentas, Madrid, Spain). Probe sequence information is provided in Table 2. ISH was performed basically as described by Ferran et al. (2015). After hybridization, the sections were washed and incubated in a solution containing alkaline phosphatase-coupled anti-digoxigenin antibody (diluted 1:3500; Roche Diagnostics). Nitroblue tetrazolium/5-bromo-4-chloro-3-indolyl phosphate (NBT/BCIP; Roche) solution was then used as chromogenic substrate for the final alkaline phosphatase

reaction (Boehringer, Mannheim, Germany). No specific signal was obtained with sense probes (data not shown).

Molecular markers listed in Table 3 were analyzed from ISH images downloaded from the Allen Brain Atlas (https://mouse.brain-map.org/; https://developingmouse.brain-map.org). The AGEA correlation option of this database was used to find genes expressed non-ubiquitously in the hypothalamic entopeduncular region mainly from E18.5 onwards (https://mouse.brain-map.org/agea and https://developingmouse.brain-map.org/agea/show). The crosshair marker was placed sequentially along diverse dorsoventral peduncular hypothalamic subdomains, either alar or basal, and the tool *Find genes* was used to obtain a list of local candidate genes of interest. We checked in detail the expression patterns of all these genes, selecting those most discriminative for our purpose. We also checked genes previously mapped in the literature that were ascribed to the entopeduncular complex (n = 49; Table 3; Wallace et al., 2017). Additionally, we analyzed *Chat* expression data on the internal globus pallidus from the Gene Expression Nervous System Atlas (GENSAT) at the Rockefeller University (gensat.org).

2. 9 Allen Mouse Brain Connectivity Atlas

We searched the efferents of the globus pallidus and the entopeduncular nuclei at the Allen Mouse Brain Connectivity image database of anterograde projections labeled by enhanced green fluorescent protein (EGFP)-expressing adeno viral (rAAV) tracers and visualized after 2–3 weeks using a serial two-photon tomography system (see Table 4 for the selected experiments).

3. RESULTS

3.1 Genoarchitectonic background

There is evidence that some mouse entopeduncular nucleus (EP) neurons express *Dlx1,2,5,6*; these genes are expressed in the telencephalic subpallium (ventricular and subventricular zone and part of the mantle zone) and have separate expression domains in the hypothalamus and prethalamus (Bulfone et al., 1993; Liu et al., 1997; Puelles & Rubenstein, 2003; Puelles et al., 2004, 2021). We explored here whether the mouse entopeduncular population (EP) originates in the hypothalamus, with or without continuity with the pallidal primordia, using transgenic mice expressing *LacZ* under control of the zebrafish *Dlx5/6* forebrain enhancer (Zerucha et al., 2000; Stühmer et al., 2002a,b). The *LacZ* histochemical reaction was compared with immunochemical reaction for several transcription factors (DLX, NKX2-1, OTP, PAX6, TBR1), calcium-binding proteins (calbindin, calretinin, parvalbumin), and *in situ* RNA hybridization reaction for *Nkx2-1*. We also examined various hypothalamic markers characterizing entopeduncular cell populations interstitial to the cerebral peduncle selected empirically and downloaded from ISH data at the Allen Brain platform (Allen Mouse Brain Atlas; Allen Developing Mouse Brain Atlas; Table 3).

We soon found that the mouse entopeduncular nucleus (EP) as classically defined consists at least of two developmentally independent, molecularly diverse, and well segregated

neuronal populations -the dorsal and ventral EP nuclei (EPD, EPV)- which are produced respectively at dorsoventrally stacked alar peduncular hypothalamic progenitor domains, the paraventricular and subparaventricular areas (Puelles et al., 2012). The basic dual nature of the mouse EPD/EPV complex is fully consistent with corresponding dual adult connectivity data (see below). In addition, we found that the entopeduncular locus intercalated between the EPD and the overlying subpallium (globus pallidus) contains two other entopeduncular cell populations which are hardly known but are molecularly distinct from the classically described components. We have named them the prereticular and preeminential entopeduncular nuclei (EP_{PRt}, EP_{PEm}) according to their position relative to neighboring prethalamic formations.

Correlative genoarchitectonic data on the mouse telencephalic globus pallidus primordium (GP) provided evidence that this entity consists primarily of at least two partially distinct parts (called here external and internal GP; GPE, GPI), which apparently derive respectively from the adjacent pallidal, and diagonal progenitor MGE subdomains (Flames et al., 2007; Puelles et al., 2013, 2016; Silberberg et al., 2016).

This insight would support the hypothesis that the observed two parts of the telencephalic mouse globus pallidus are the developmental and topological homologs of the external and internal pallidal segments of primates. The novel EP_{PRt} and EP_{PRm} nuclei at the telencephalic stalk region separate the GPI from the classic hypothalamic EP (specifically from the EPD and underlying EPV).

We will first describe our results on the mature topography of the different parts of the entopeduncular complex (EPV, EPD, EP_{PRt}, EP_{PEm}) and the respective molecular marker profiles they exhibit at postnatal stages of mouse development. Next, we will examine the origin of these nuclei out of ventricular zone domains identifiable at early stages (starting at E11.5 and with emphasis in the classic EPV/EPD components, object of the discussed homology hypothesis). In a subsequent section, we will provide selected data on the existence of two distinct globus pallidus subdomains in the mouse telencephalic subpallium.

3.2 Organization of entopeduncular cell populations at mature stages

We found four ventrodorsally arranged hypothalamic cell aggregates disposed interstitially to the cerebral peduncle, the ventral, dorsal, prereticular and preeminential entopeduncular nuclei, each showing a different molecular profile (EPV, EPD, EP_{PRt}, EP_{PEm}; Figures 1, 2, 3; Table 3). They are clearly distinguishable in sagittal sections.

We understand the cerebral peduncle as a strictly transverse (dorsoventral) tract that first emerges from the telencephalic subpallium at the telencephalo-hypothalamic transition area, then courses through the peduncular hypothalamic alar domain (where it incorporates ascending thalamic components), penetrates the underlying basal plate region alevel with the subthalamic nucleus, and finally bends caudalwards into the diencephalic tegmentum (pe; Figure 3b).

The alar peduncular hypothalamus is divided dorsoventrally between the *Dlx*-negative paraventricular area and the *Dlx*-positive subparaventricular area (Puelles & Rubenstein, 2003; Puelles et al., 2012, 2021; Diaz et al., 2023; Figure 1a).

The EPV is clearly identified by its strong *Dlx5/6-LacZ* signal interstitial to the peduncle in a postnatal brain from a transgenic *Dlx5/6-LacZ* mouse line (blue labelling in Figures 1b–d; see also Figures 2j,k). It also expresses *Nkx2-1*, a feature shared with pallidal formations (EPV; Figure 2b). EPV cells appear to be GABAergic since they express *Gad1* and the vesicular GABA transporter *Slc32a1* (Table 3). Several other mRNA transcripts typically characterizing the EPV include the transcription factors *Arx*, *Foxp2*, and *Meis1*, and other genes such as *Cbln2*, *Chrm3*, *Pvalb*, *Trpc4, Rgs4,* and *Spp1* (Figures 2a,b; Table 3). The EPV is typically aligned dorsoventrally within the *Dlx*-positive subparaventricular band (in longitudinal continuity with the recently defined rostral liminar nucleus -RLi- of the prethalamus, which is also *Dlx5/6-LacZ* positive; Puelles et al., 2021; Diaz et al., 2022; EPV, RLi; Figure 1a). The peduncular position of EPV typically coincides roughly with the subpial course of the optic tract (ot; Figures 1c, 3), and is somewhat dorsal relative to the STh nucleus in the underlying **basal plate** (Figures 1b–d, 2b,k) and ventral to its alar companion, the EPD (the optic tract is thus useful for the distinction of the neighboring EPV and EPD formations). The basal STh is *Dlx*-negative and stands out from surrounding structures by its strongly calretinin (CR)-positive neurons and neuropile; it lacks otherwise PAX6- and calbindin (CB)-immunoreaction (STh; Figure 1).

The EPD and EP_{PRt} are both devoid of *Dlx* related signals and are rostrally aligned with the incertal and reticular prethalamic complexes, respectively (Figure 1).

EPD is distinguishable by its selective PAX6 and calbindin (CB)-positive immunostaining (Figures 1A,B,D), and expresses *Pax6*, *Tbr1*, *Cyp26b1* and *Nr2f1* (Figures 2d,e,h), among other genes noted below (see also Table 3). Contrarily to the GABAergic character of EPV, the EPD is glutamatergic; it expresses *Slc17a6* mRNA (Figure 2f; Table 3) that encodes a vesicular glutamate transporter (vGLUT2) (Takamori et al., 2000). The EPD lies superficially in the wholly *Slc17a6*-positive paraventricular domain mantle (Figure 2f); it neighbors caudally with the prethalamic zona incerta complex (EPD; ZI; Figures 1b,c,3) and ventrally with the underlying subparaventricular domain where the EPV lies; these caudal and ventral neighboring entities are *Slc17a6*-negative (ZI; Figure 2f). Other markers that label selectively EPD cells are the transcription factors *Barhl2*, *Pbx3, Pou2f2* and *Zfnx3,* the neuropeptide somatostatin *(Sst),* and other genes such as *Cacna2d1*, *Cbln4*, *Crtac1*, *Synpr*, and *Stbp6* (Table 3).

In contrast, EP_{PRt} is PAX6- and CB-negative (Figures 1a,b,d) and expresses *Isl1* and *Cacna2d3,* markers absent at EPD (though EP_{PRt} shares expression of *Nr2f1* with EPD; Figures 2g–i). The prethalamic reticular nucleus complex (Rt), from where EP_{PRt} neurons may migrate, is also labeled with these molecular markers; however, we found some differences such as *Enc1* whose signal labels the EP_{PRt} but not Rt (Allen Developing Mouse Brain Atlas; see also Puelles et al., 2021). Additional molecular markers such as *Cdh6*, *Ecel1*, *Esrrg*, *Kitl*, *Meis2,* and *Six3* also characterize specifically this EP_{PRt} population (Table 3). Our P0 sections double-labelled for *Dlx5/6-LacZ* (Xgal) and pan-distalless IHC

show that at this stage EP_{PRt} is negative for *Dlx5/6-LacZ* expression, but positive for the pan-distalless antibody (DLX; brown reaction; Figures 2j,k). This combination was interpreted in Puelles et al. (2021; see their Discussion) as indicating selective postnatal expression of *Dlx1/2* (after downregulating *Dlx5/6*).

Finally, the pre-eminential EP nucleus (EP_{PEm}) is associated topographically to the transitional telencephalo-opto-hypothalamic domain (Morales et al., 2021), which is *Dlx*- and *Nkx2-1*-negative and corresponds to the ventralmost *Foxg1*-positive telencephalic domain. These cells are found in an entopeduncular location in the upper subregion of the paraventricular area (Figure 2l).

A fifth or extra entopeduncular cell group termed by us ‘accessory entopeduncular nucleus’ (EPA; Puelles et al., 2021) is represented by a small strongly *Dlx-LacZ*-positive aggregate that lies outside the hypothalamus, interstitial to the incipient longitudinal peduncular course through the prethalamic tegmentum, and ventrocaudal to the peduncular bend around the STh (EPA, STh; Figures 1c,d; 2k). The differential topographic location of the *Dlx*-positive EPA and EPV nuclei is clearly visualized by combination of calretinin (CR) and calbindin (CB) IHC at early postnatal stages; the STh contains CR-positive and CB negative cells (STh; Figures 1c,d). The CB-positive EPD and the *Dlx*-positive EPV are embedded specifically within the transverse entopeduncular trajectory of the CB-positive *ansa lenticularis* tract, one of the descending components of the cerebral peduncle, whereas the *Dlx*-positive EPA lies interstitial to the longitudinal course of the entopeduncular ansa lenticularis (al) once this tract bends superficially caudalwards around the *Dlx*/CB-negative and CR-positive subthalamic nucleus (Figures 1c,d). Both EPD and EPV are thus alar hypothalamic, whereas EPA seems diencephalic (prethalamic) and tegmental (Ramon y Cajal, 1903, and Watanabe & Kawana, 1982, identified it as ‘accessory subthalamic nucleus of Luys’; Talbot & Butcher, 1978 and Marchand & Lajoie, 1986 named it ‘nucleus of the crus cerebri’; Puelles et al., 2021 called it ‘accessory entopeduncular nucleus’). Besides the *Dlx* signal, EPV and EPA share the expression of markers such as *Arx, Cbln2, Chrm3*, *Foxp2, Gad1*, *Pvalb*, *Nkx2-1*, *Slc32a1*, and *Trcp4* (Figures 2a,b; Table 3), consistent with a GABAergic profile of both populations.

In summary, our analysis of entopeduncular cell groups associated with the hypothalamic course of the cerebral peduncle, based on the Allen Developing Mouse Brain ISH database and our own genoarchitectonic data, contributes to a more complete characterization of a set of four alar entopeduncular cell populations of the PHy. The EPV is topographically related to the *Dlx*-positive hypothalamic subparaventricular domain (rostral to the RLi formation; EPV, RLi; Figures 1a,2,3; see Puelles et al., 2021). The EPD subdivision is found immediately dorsal to the EPV. This population lacks *Dlx5/6-LacZ* and calretinin (CR) protein, displaying instead calbindin (CB/*Calb1*) (Figures 1d; Table 3), PAX6/*Pax6* (Figures 1a,b, 2c; Table 3), *Tbr1*, *Cyp26b1,* and *Nr2f1*, among others (Figures 2d,e,h; Table 3) in its profile.

Located dorsal to EPD, the EP_{PRt} was previously described as a transient *perireticular* nucleus in rat and ferret embryos (Mitrofanis, 1992, 1994a,b; Earle & Mitrofanis, 1996), though dispersed cells with identical topography appear immersed in the cerebral peduncle

dorsal to the EPD and rostral to the prethalamic reticular complex postnatally (PRt; Figs.2g–k, 3). Considering its location rostral to the prethalamic reticular complex we propose that the *prereticular* term is appropriate for this cell population (Puelles et al., 2021). We hypothesize that these DLX-positive (i.e., DLX1/2 positive stainable with pan-distalless antibody), and thus probably GABAergic cells, may originate via tangential migration from the prethalamic reticular complex (an alternative possible source might be the preoptic area). The *Isl1*-positive EP_{PRt} population appears as rows of dispersed cells among the peduncular fibers at levels where the thalamic peduncle incorporates (PRt; Figure 1i).

Finally, at the transition into the *Foxg1*-expressing telencephalic territory (Morales et al., 2021), the EP_{PEm} population contains differentially *Foxg1*-expressing cells reported to be largely glutamatergic (Figure 2l; Morales et al., 2021).

In the Discussion the relationship of these entopeduncular hypothalamic nuclei with the internal and external globus pallidal subdivisions (GPI, GPE) in the neighboring subpallial region will be considered, jointly with their hodologic similarities and differences.

3.3 Early histogenetic domains

Our analysis of the relative postnatal topography of diverse *Dlx5/6-LacZ*-positive cell populations in the peduncular forebrain suggested that the EPV might originate in a *Dlx*-positive progenitor domain within the embryonic peduncular hypothalamus at levels roughly covered by the optic tract (see Fig.1C). The obvious candidate domain corresponds to the peduncular part of the subparaventricular band characterized by *Dlx5/6-LacZ*-positive periventricular cells that, as a whole, extends longitudinally across the hypothalamus between the rostral anlage of the suprachiasmatic nucleus and the subincertal RLi area of the prethalamus in prosomere 3 (SPa; Puelles et al., 2012; the subparaventricular term was introduced by Watts & Swanson, 1987; Watts et al., 1987). This band is held to represent the ventral rim of the hypothalamic alar plate through both hypothalamic prosomeres hp1 and hp2. The peduncle only crosses its hp1 or peduncular part (thus ‘peduncular SPa’ or PSPa; Figure 4a; ‘posterior entopeduncular area’ in Puelles & Rubenstein, 1993; 2003). The SPa lies just ventral to the paraventricular histogenetic area (Pa), the dorsal alar source of magnocellular hypophysiotropic neurons, where *Dlx5/6-LacZ* is not expressed (Pa; Figure 4a). The SPa domain displays a relatively massive rostral part in the terminal hypothalamus (TSPa; encompassing the anterior hypothalamic and suprachiasmatic grisea) and caudally a thinner peduncular part (PSPa; Figure 4a). The PSPa displays superficially the peduncular fibers with the EPV, underlined by a molecularly distinct lateral hypothalamus sector (Diaz et al., 2023), and its periventricular stratum is dorsoventrally thin (Figure 4a). The PSPa is continuous caudally with the *Dlx5/6-LacZ*-positive primordium of the prethalamic liminar band in prosomere 3, which borders ventrally the zona incerta, from which it was not distinguished by classic neuroanatomists (PSPa, RLi; Figures 4a–c). We hold that this PSPa domain represents the main source of the *LacZ*-expressing EPV cells (see evidence below).

On the other hand, the progenitor domain for the neighboring *Dlx5/6-LacZ*-negative EPD lies in principle just dorsal to the PSPa. The obvious candidate would be the *Dlx*-negative, *Otp*-, *Pax6*- and *Tbr1*-positive paraventricular hypothalamic domain, which lies rostral to the prethalamus (Figures 1,2D; 4a,d; Table 3; Bulfone et al., 1993, 1995; Puelles & Rubenstein,

1993, 2003; Simeone et al., 1994; Fan et al., 1996; Martínez & Puelles, 2000; Puelles et al., 2004, 2012). We turned to embryonic material to test these hypotheses.

3.4 Embryonic development of EPV

The *Dlx5/6-LacZ*-positive thin peduncular subparaventricular zone (PSPa) is well-distinguishable in sagittal sections at E13.5 (Figure 4a). It is already present periventricularly at E11.5 (Figure 4c). It ends caudally at the rostral limit of prosomere 3, whose central and subcentral alar prethalamic territory (the old ventral thalamus) characteristically contains a larger dorsoventral expanse of *Dlx* expressing cells (p3, PTh; Figure 4a; see also Puelles et al. 2021; their Fig. 1b). As recently shown in Puelles et al. (2021), the central PTh subdomain forms the reticular nucleus, whereas the subcentral subdomain generates the zona incerta and the underlying rostral liminar band (Rt, ZI, RLi; Figure 4a). At E11.5 we could not identify a separate EPV cell group in relation to the incipient peduncular mantle stratum (pe; Figures 4b,c), though these early *LacZ*-positive PSPa cells probably represent the prospective EPV, given the reported outside-in generation pattern (Wyss & Sripanidkulchai, 1985).

At E12.5, horizontal and transverse sections through the PSPa show an incipient group of *Dlx5/6-LacZ*-positive cells already in an entopeduncular position (arrows in Figures 4f,o–q,5c). This entopeduncular aggregate is better developed at E13.5 (Figures 4G,5D) and the EPV primordium displays in sagittal sections a characteristic topography dorsal relative to the migrated primordium of the subthalamic nucleus (EPV; STh; Figures 5h,i). Additional *LacZ*-positive cells may originate in the underlying basal retrotuberal hypothalamic area under the subpial STh primordium, which possibly contribute *Nkx2-1* cells to EPV (asterisk; RTu; Figures 4p–r). Moreover, the TSPa does not show a comparable superficial cell group, nor do peduncular fascicles grow through it (Figure 4j–l).

By E15.5 the *LacZ*-positive EPV nucleus appears established as a well-defined compact mass in its definitive position, close to the dorsoventral level marked superficially by the optic tract (Figure 4h). At later stages, further growth of the peduncle confers a slightly reticular appearance to EPV (Figures 5k–m).

The earliest *Nkx2*-1 expressing cells at the EPV primordium were observed at E12.5 and E13.5 (Figures 5f,g,i,j,). In general, this marker distributes throughout the basal and floor ventricular and mantle zones of the hypothalamus and prosomere 3, with exception of the retromamillary area and its derivatives (i.e., the STh; Figures 5f,i). A distinct but rather thin subparaventricular band of *Nkx2-1*-expressing cells overlaps specifically the lower part of the *Dlx*-positive TSPa/PSPa in the mantle layer, parallel to the dorsal border of the hypothalamic basal-plate expression domain (Figures 5f,g,n; compare also Figures 4h and 4i at E15.5). Similar thin domains of overlap with *Dlx* expression in PSPa were identified as well using *Nkx2-2*- and *Nkx5-1*-ISH reactions (not shown). Superficial entopeduncular *Nkx2-1*-, *Nkx2-2*- and *Nkx5-1*-positive cells were seen likewise at the EPV primordium, forming a subset of the *LacZ*-positive neurons, mixed with cells that express only *Dlx5/6-LacZ*, probably originated at the more dorsal part of the PSPa (Figures 5a–d, n–p).

3.5 Embryonic development of EPD

Examination of similar E12.5-E13.5 *LacZ* material counterstained with immunoreaction for either PAX6 or TBR1 proteins as well as E11.5-E15.5 *Tbr1* ISH data from the Allen Developing Mouse Brain Atlas showed that these markers are characteristic of the mantle layer of the neighboring *Dlx*-negative paraventricular area (PPa), which lies immediately dorsal to the PSPa (Fig.6). The ventricular zone of this histogenetic domain (Bulfone et al., 1993) is known to express the PAX6 transcription factor early on (Puelles et al., 2012; Figures 5e,h). Calbindin, another EPD marker, is also expressed strongly in the primordia of the supraoptic nucleus and the paraventricular nucleus, both formed within the Pa, but not in the adjoining *Dlx*-positive mantle domains (not shown).

At E11.5, *Tbr1*-expression also labels massively the prethalamic eminence just caudal to the PPa domain (PThE; Figures 6a,b; characteristically, PAX6 appears selectively only in the eminential ventricular zone - Figures 1a, 5e,h-, whereas Tbr1/TBR1 is expressed in its mantle zone -Figures 6a–h; Bulfone et al., 1995). This expression pattern thereafter extends rostralward into the PPa area and its *Dlx5/6*-negative mantle domain (Figures 6c, e–m; Bulfone et al., 1995). The TBR1-expressing PPa mantle domain is accordingly wedged between the *LacZ*-positive subparaventricular band (ventrally) and the *LacZ*-positive subpallial complex (dorsally) (compare Figure 5e and Figure 6h; Puelles & Rubenstein, 2003). Paraventricular $TBR1^+$ IHC encompasses distinctly the superficial EPD cells which lie directly dorsal to the *Dlx*-positive EPV primordium (Figures 6h–n). The *LacZ*-negative EPD appears labelled as well with ISH for *Otp* at E12.5 (Figure 4d); OTP is a transcription factor crucial for the differentiation of the neuronal phenotypes developing within the Pa area, which is absent at the prethalamic eminence (Simeone et al., 1993; Acampora et al., 1999; Wang & Lufkin, 2000).

Other early markers of the prethalamic PThE and the neighboring hypothalamic PPa (including EPD) are *Barhl2*, *Cacna2d1*, *Pbx3*, *Pouf2f2*, *Zfhx3* and *Slc17a6* (encoding vGLUT2) (Allen Developing Mouse Brain Atlas).

3.6 Embryonic development of EP_{PRt}

The EP_{PRt} appears initially in continuity with the rostralmost part of the DLX-positive prethalamic reticular nucleus, from which its cells seem to originate (Earle & Mitrofanis, 1996; Mitrofanis, 1994a,b; Puelles et al., 2021; Zhao et al., 2008;). However, these elements later downregulate *Dlx5/6*, retaining mainly *Dlx1* signal (Puelles et al., 2021), and thus appear as a *Dlx*-*LacZ*-negative but nevertheless pan-DLX-immunoreactive cell population lying dorsal to EPD and rostral to the reticular complex from E13.5 onwards (Figures 1a–c, 2j,k). Another marker of EP_{PRt} and prethalamic Rt cells is the *Isl1* transcription factor (Figure 2i). We have mapped *Isl1* expression in material from the Allen Developing Mouse Brain Atlas examining sagittal and horizontal sections through the hypothalamus and prethalamus between stages E11.5 and E18.5 (Figure 7). At E11.5, *Isl1* is strongly expressed only in alar PTh cells. Moreover, the *Dlx*-positive hypothalamic subparaventricular domain and the basal hypothalamus also display strong *Isl1* signal whereas the alar hypothalamic paraventricular domain lacks *Isl1* expression (Figures 7a,b). At E12.5, a few *Isl1*-positive cells are found superficially to the peduncle in the prereticular sector of the hypothalamus;

we interpret these cells as possibly tangentially migrated elements of the EP_{PRt} primordium (Figure 7c, arrow). At E13.5, there is an increase in the number of such superficial *Isl1* cells (Figures 7d,e). At E15.5, this population is no longer superficial but interstitial to the fibers of the cerebral peduncle, probably due to incorporation of additional peduncular fiber contingents (Figures 7f,g). This emergent EP_{PRt} topography is clearer at E18.5 (Figures 7h,i).

3.7 Development of the EP_{PEm}

Our data on a developing *Foxg1*-positive EP_{PEm} primordium dorsal to the EP_{PRt} is limited to E18.5 (Figure 2l). Unfortunately, available Allen material from earlier stages is restricted to sagittal sections and does not allow the separation of this entopeduncular population from the neighboring subpallium. Morales et al. (2021) showed in their E12.5 *Foxg1* material some positive cells lying superficial to the peduncular tract labelled as ‘internal capsule’ (their Fig.2f). This suggests a possible developmental pattern analogous to that of EP_{PRt} but originated in the *Foxg1*-positive telencephalo-opto-hypothalamic domain.

3.8 Collateral observations on globus pallidus

Distinct subpallial GPI and GPE formations are clearly identified postnatally in the mouse based on *Dlx5/6-LacZ*, *Lhx8*, and *Nkx2-1* expression (Figures 8a–j). Both GPE and GPI lack TBR1 and PAX6 immunolabelling (Figures 8c, e, h). The adjacent striatal complex is *Dlx5/6*-LacZ-positive but NKX2-1-, *Lhx6*-, and *Lhx8*-negative (Figure 8; see also Medina & Abellán, 2012; their Figs. 7.9). GPI cells are relatively larger and more dispersed neurons that strongly express *Dlx*5/*6-LacZ* within a roughly triangular caudomedial area of the GP complex (Figs. 8b–g), which is caudally continuous with the nucleus of the ansa lenticularis (AL; Figures 8e–g); note all these AL cells are cholinergic in the adult, thus being supposedly derived from the basal telencephalon (Gould et al., 1991; Oh et al., 1992). The *Lhx8* marker, present in both GPE and GPI, also illustrates the cytoarchitectonic difference between the GPE and GPI cell types (Figure 8a). The smaller and more compact postnatal GPE neurons show less *Dlx*-expression compared to earlier stages (see Figures 1b,d), and display among other differences a relatively weaker *LacZ* signal compared to GPI (Figures 8b–f; i,j). In contrast, there is much stronger *Nkx2-1*/NKX2-1-expression in GPE than in GPI (Figures 2b; 8b,d,g). GPI shows as expected a substance P-immunopositive neuropil, indicating specific striatal afferents (Figure 9a). In the adult brain, a tyrosine-hydroxylase (TH) positive fiber plexus is restricted to the GPI neuropil (Figure 9b), whereas GAD- and PV-immunoreaction is relatively stronger within GPE than in GPI (Figures 9c,d). Moreover, we observed in GPE relatively numerous *Spp1*-positive cells (Figure 8e), as well as other markers such as *Cyp26b1, Ecel1, Enc1, Esrrg, Gabra5, Gabrg1, Meis2, Oprl1, Plcl1* and *Stxbp6* (Table 3); Interestingly, *Cyp26b1, Gabra5, Gabrg1,* and *Plcl1* expression characterizes selectively both the subpallial GPE and the hypothalamic EPD, which appears separated by a negative domain containing the GPI; contrarily, *Cdh6* and *Ecel1* signals characterize selectively both GPI and EP_{PRt} cells. *Chat*, *Ecel1* and *Slc18a3* label specifically a sizeable subpopulation of GPI cells displaying a cholinergic profile, similar to that seen at the more caudal, tail-like AL nucleus. This cell type also partly disperses into the neighboring GPE, the diagonal band nucleus and medial septum, and the local internal capsule (Figures 9f–h; *Slc18a3* encodes a vesicular monoamine transporter).

Other markers such as *Nxph4,* and *Nr4a2* are selectively expressed in a subpopulation of GPI cells (the latter best seen at E15.5 and E18.5; check the Allen Developing Mouse Brain Atlas), whereas *Oprl1* and *Pclc1* signals characterize selectively the GPE (Table 3). Other markers such as *Arx*, *Chrm3* and *Cbln2* label both the subpallial GPI and the hypothalamic EPV, whereas the transcription factor *Pbx3* appears in both GPI and EPD cells (Table 3).

Within our model of subpallial areal structure (Puelles et al., 2013, 2016) the GPE is postulated to be an intermediate mantle stratum within the *central pallidal* progenitor domain (correlative periventricular and superficial central pallidal formations being the lateral part of the periventricular BST complex and the rostral moiety of the substantia innominata, plus a rostral part of the subpial diagonal band (Figure 8j); formerly a part of the olfactory tuberculum [Tu] was assigned to superficial pallidum, but we now consider the Tu proper as uniformly striatal in origin, though it contains tangentially migrated pallidal cells in its deep stratum). The GPI is held to form instead the parallel intermediate stratum of the *central diagonal* progenitor domain (*loc.cit.*). The central diagonal radial domain includes deep to GPI the medial part of the BST complex, and, superficially the posterior moieties of the substantia innominata and the superficial diagonal band (SI_{PAL},DB_{PAL},SI_{Dg},DB_{Dg}; Figures 1b; 8j).

Analysis of successive stages of development suggests that our *diagonal subpallial progenitor domain* (Dg; equivalent to our old ‘anterior entopeduncular area’, AEP; Bulfone et al., 1993; Puelles & Rubenstein, 1993; Rubenstein et al., 1994) contributes to the internal (caudomedial) part of the classic globus pallidus (see preliminary observations in Flames et al., 2007; Puelles et al., 2016; Silberberg et al., 2016) where it develops jointly with medial BST subnuclei, posterior substantia innominata and part of the diagonal band nuclei (Puelles et al., 2013; 2016). Medina and Abellán (2012) identified our Dg (AEP) subpallial domain as ‘caudoventral pallidum’, their criterion being conditioned by the initial absence of differential diagonal versus pallidal markers. This argument seems now superseded by our present data in Table 3. Many cells generated in this singular subpallial territory are GABAergic as occurs in other subpallial entities, correlative with the shared *Dlx5/6-LacZ*, *Lhx6* and *Lhx8* signals, irrespective of the apparent local origin of the cholinergic neurons of the basal forebrain (Figures 8a–f; Shimamura et al., 1997; Eisenstat et al., 1999; Puelles et al., 2000; Marin et al., 2002; Flames et al., 2007; Long et al., 2009; Zaborszky et al., 2012; Su-Feher et al., 2022).

3.9 Pallidal and entopeduncular connectivity

We examined data from eight efferent mapping experiments performed in mouse by injecting recombinant adeno-associated virus (rAAV) into the pallidal and entopeduncular regions (Allen Mouse Brain Connectivity Atlas). After two injections on C57CL/6J mice centered essentially in our postulated GPI (cases 158373958 and 300318924, curiously also identified as GPI in the Allen source), we found distinct anterograde labeling in the thalamus (i.e., ventral anterior, ventral lateral, mediodorsal and parafascicular thalamic nuclei; supplementary Figures S1a–e); additional terminal labeling was detected in the EPV (Figure S1d), STh (Figure S1e), substantia nigra pars reticulata (SNr) and pretectum (PT) (not shown). In contrast, two other experiments with injections centered strictly in

GPI, but done in *Ntrk1-IRES-Cre* mice, showed wide anterograde labelling selectively in the neocortex (cases 647574144 and 265944167; Figures S1f,g), the lateral amygdala, prethalamic eminence and reticular nucleus (not shown). The *Ntrk1* gene encodes a member of the neurotrophic tyrosine kinase receptor family which plays a critical role in proliferation and differentiation of cholinergic neurons (Li et al., 1995). Thus, the *Ntrk1-IRES-Cre*-dependent labelling produced in these two experiments represent selectively cholinergic projections originated in the cholinergic neurons lying within GPI.

Two rAAV injections into the EPD gave rise to labeled fibers in the stria medullaris and terminals in the lateral habenula (cases 305024724 and 539498984; Figures S1h,i). Other EPD efferents end in basal parts of the lateral hypothalamus (bHL), the prethalamic subgenigulate nucleus, the ventromedial thalamic nucleus (VM) and the pretectum (PT) (Figures S1h,i). We did not identify experiments centered upon the EPV.

4. DISCUSSION

Present data reveal that the mouse cerebral peduncle contains at least three extratelencephalic and one telencephalic entopeduncular cell populations, each one characterized by a different combination of molecular markers. They are the ventral and dorsal entopeduncular nuclei (EPV, EPD), classically conceived jointly as a single entopeduncular population, plus the newly identified prereticular entopeduncular nucleus (EP_{PRt}), to which we add the telencephalic preeminential entopeduncular nucleus (EP_{PEm}), as illustrated in Figures 3 and 10a. The EPD, EP_{PRt} and EP_{PEm} populations correlate topographically with different dorsoventral parts of the *paraventricular* alar hypothalamic area, whereas the EPV is a superficial component of the subjacent *subparaventricular* alar hypothalamic area (Puelles et al., 2012); note that hypothalamus literature based on the columnar model does not recognize the subparaventricular area as defined by Puelles et al. (2012), which encompasses rostrally the GABAergic classic anterior hypothalamic and suprachiasmatic nuclei. The subparaventricular domain was otherwise recently referred to as ‘diagonal hypothalamic area’ by Shimogori et al. (2010). This descriptor is due to debatable combined reference to both columnar and prosomeric axes (being mutually orthogonal at this locus, they define a bisecting diagonal if one accepts both; this is meaningless from a causal viewpoint, since only one axis can have acted). Recently the EPD and EPV entopeduncular populations have been differentiated molecularly and hodologically in the mouse adult brain, without being assigned specific names (rostral and caudal EP parts of Miyamoto & Fukuda, 2015, 2021a,b; Wallace et al., 2017;). Using Herrick’s columnar model, which defines the hypothalamus as a longitudinal column, these authors distinguished a ‘caudal’ parvalbumin immuno-reactive cell population (our EPV) from a ‘rostral’ parvalbumin-negative and somatostatin-positive cell population (our EPD). The EP_{PRt} cells are usually interpreted as a transient ‘perireticular’ cell population found within the internal capsule in rat and ferret embryos, which is reduced postnatally (Mitrofanis, 1992, 1994a,b; Mitrofanis & Baker, 1993;Mitrofanis et al., 1995; Earle & Mitrofanis, 1996). The EP_{Pem} is a superficial entopeduncular component found at the dorsal part of the paraventricular domain, which was recently identified as a Dlx- and Nkx2-1-negative telencephalo-opto-hypothalamic area whose *Foxg1*-expressing cells are

mainly glutamatergic (Morales et al., 2021; *Foxg1* is held to be a telencephalon marker) (Figure 2l).

The two main subdivisions currently noted within the classic EP entity display distinct molecular heterogeneity and little mutual overlap in other features. The EPD cells are *Dlx5/6-LacZ* negative and express transcription factors such as *Tbr1*/TBR1, *Pax6*/PAX6, *Otp and Nr2f1,* jointly with some other markers such as *Cacna2d1*, *Calb1*/calbindin CB, *Crtac1, Cyp26b1*, *Nos1*, and *Sst* (Table 3). Unlike the EPD, the EPV cell population is intensely *Dlx5/6-LacZ* positive and expresses GABAergic markers (*Gad1*/*Gad67*, *Slc32a1*, *Pvalb*/parvalbumin PV) as well the transcription factors *Arx*, *Foxp2, Meis1* and *Nkx2-1* (Table 3). The EP_{PRt} contains selectively *Ecel1*, *Isl1*, *Meis2*, and *Kitl*-expressing cells, among other markers, whereas EP_{PEm} cells uniquely express the transcription factor *Foxg1* (Table 3).

4.1 On the alar hypothalamic origin of EPV

The presently described *Dlx5/6-LacZ* positive EPV appears to originate from a caudal (peduncular) portion of the *Dlx5/6-LacZ*-positive subparaventricular area (PSPa; Puelles et al., 2012; this particular area was formerly tentatively identified as ‘posterior entopeduncular’ or PEP by Bulfone et al., 1993 and Puelles & Rubenstein, 1993, previous to the more detailed hypothalamic structural descriptive analysis of Puelles et al., 2012). In *Dlx5/6*-LacZ material, the positive PSPa domain is continuous caudally with the recently identified *rostral liminar band* of the prethalamus (RLi; Puelles et al., 2021; Diaz et al., 2023). The ontogenetic and adult location of EPV at dorsoventral peduncular hypothalamus levels roughly under the subpial optic tract obviously make its generation independent of the distant developmental origins of the pallidal subpallial telencephalic primordia. Importantly, we did not observe in our embryonic series any *Dlx*5/6-*LacZ*-positive migratory stream that interconnects these two independent sources of *Dlx5/6-LacZ* positive neurons at any stage during development.

The neuroepithelial origin we assign to EPV agrees roughly with that attributed by some previous authors to the entire entopeduncular complex (Gilbert, 1935; Papez, 1940; Keyser, 1972, 1979; Marchand & Poirier, 1983; Marchand & Lajoie, 1986; Bayer, 1985); these authors lacked a specific marker for this cell population and apparently did not suspect a dual origin and nature of EPV/EPD. We were initially able to distinguish EPD from EPV in our material by *Dlx5/6-LacZ* expression specific to the EPV,

Dlx-family genes and *Nkx2-1* are characteristic joint markers of the EPV neurons, which are co-expressed early on in a ventral part of the PSPa (Figure 5). Relevant *BF2* (*Foxd1*) data of Hatini et al. (1994) suggest EPV expression of this subparaventricular-selective marker (similarly as *Meis1*; Table 3), adding support to our PSPa origin hypothesis for EPV.

We were surprised that NKX2-1-expressing neurons are also present in the EPV, since we initially assumed that this gene is a selective marker for basal plate derivatives of the hypothalamus, whereas the subparaventricular area develops at the ventral rim of the alar plate (Bulfone et al., 1993; Puelles & Rubenstein, 2003). Our present more detailed observations, partly including double-labeled material, suggest that there is at least partial

expression overlap at the subparaventricular mantle of *Dlx5/6* and *Nkx2-1*, and this overlap is reflected in the EPV. An ancient and subsequently reduced alar hypothalamic expression of *Nkx2-1* was discussed in the context of brain evolution in *Xenopus* (van den Akker et al., 2008). Alternatively, a dorsal migration of NKX2-1+ EPV neurons from the basal plate into the alar subparaventricular band may be considered.

It is remarkable that the molecular profile of the mouse EPV cells significantly resembles that of the mouse internal globus pallidus (GPI). Both share *Dlx family genes*, *Arx*, *Chrm3*, *Cbln2*, *Nkx2-1, parvalbumin (Pvalb*/PV*),* and GABAergic markers (*Gad1*, *Slc32a1*). Furthermore, both the diagonal subpallial subventricular zone (Dg) that apparently generates the internal part of the globus pallidus and the peduncular subparaventricular hypothalamic progenitor area (PSPa), representing the apparent EPV origin, are *Dlx*-positive alar domains that lie adjacent to a *Shh*-positive progenitor domain. In the telencephalon, *Shh* is expressed in the ventricular zone of the neighboring preoptic area (Bardet et al., 2010; Puelles et al., 2016; see the notion of ‘subpallial organizer’ in Puelles, 2017 and Puelles et al., 2019), whereas *Shh* is separately expressed longitudinally in the hypothalamic basal plate just ventrally to the *Dlx*-positive SPa area (Shimogori et al., 2010; Puelles et al., 2012). Moreover, the *DM20 (Plp1)* gene, a marker of oligodendrocyte progenitors, is expressed in the ventricular zones of both the telencephalic Dg and the hypothalamic PSPa domains (Timsit et al., 1992; 1995; their Figs.2A,B,D). A further curious molecular parallelism between the EPV and GPI is that both arise in domains that express *Lhx6* and *Lhx8*; these ‘pallidal’ transcription factors are also expressed in a band overlapping the lower part of the PSPa and neighboring retrotuberal hypothalamic loci (Shimogori et al., 2010; their Figs.3e,4; Puelles et al., 2012; Kim et al., 2021; see the Allen Developing Mouse Brain Atlas).

There accordingly exists a remarkable *similarity* of the molecular profiles of these topologically distinct forebrain domains and derivatives; however, there is no true genoarchitectural identity (reflecting their differential forebrain positions) since at least *Isl1, Meis2* and *Nkx2-2* are differentially expressed in the PSPa, being absent at the GPI (Table 3). Such partial similarity probably underlies causally the parallel neuropharmacological phenotype (GABAergic) as well as some hodological properties (thalamic projections) of EPV neurons, which are comparable in primates and rodents GPI neurons (Figure 10; see below). This exceptional circumstance may have supported the imprecise prevailing opinion that the ‘EP’ of rodents is homologous to the GPI of primates.

Interestingly, the hypothalamic EPV component has shared hodological properties with GPI subpallial derivatives of the medial ganglionic eminence. It apparently is the main entopeduncular cell group that has projections to the motor thalamus (Kha et al., 2000, Dudman & Gerfen, 2015) whereas the EPD largely projects to the lateral habenula (Kim et al., 1976; van der Kooy & Carter, 1981; Parent & Bellefeuille, 1982; Parent et al., 1984, 2001; Heimer et al., 1991; Rajakumar et al., 1993; Barroso-Chinea et al., 2008; Hong & Hikosaka, 2008; Shabel et al., 2012; Wallace et al., 2017; Miyamoto & Fukuda 2021). Interestingly, EPV selectively receives input from the striatal matrix, similarly as the GPI, while the EPD has striosomal inputs (Rajakumar et al., 1993). Ample evidence that primates have ‘pallidal’ neurons which project to the lateral habenula and lie rather outside the GPI

and within the peduncle supports the existence of a distinct EPD formation in primates next to the GPI.

4.2 On the origin of EPD

Most previous literature held the entopeduncular nucleus of rodents to be developmentally unitary, though recent hodological results cited above demonstrate the independent existence of the presently described distinct EPD and EPV parts. In our material, the EPD expresses selectively *Calb1*/calbindin (CB), *Otp*, *Pax6*/PAX6 and *Tbr1*/TBR1 and its cells show a glutamatergic profile (consistent with our topographic description associating it to the *paraventricular area*); there are other specific molecular markers of EPD, such as *Cyp26b1*, *Nos1*, and *Sst* (Table 3; Puelles et al., 2021). Calbindin and *Otp* are markers shared by the supraoptic and paraventricular nuclei, which also derive from the *paraventricular area* (Pa; Morales-Delgado et al., 2011, 2014; Puelles et al., 2012; Diaz et al., 2015; Diaz & Puelles, 2020). The Pa ventricular zone expresses PAX6 at early stages and sharply lacks expression of the *Dlx1/2/5/6* or *Nkx2-1* genes, which are otherwise present in the neighboring subpallial, preoptic and subparaventricular domains. As noted above, the EPD cells generally express *Slc17a6*, a gene that encodes the VGLUT2 transporter, indicating a glutamatergic nature (see Puelles et al. 2012). These findings on the EPD neurons are consistent with a possible origin within the paraventricular (Pa) histogenetic area corresponding specifically to the peduncular (hp1-derived) alar hypothalamus (Puelles & Rubenstein, 2003; Puelles et al., 2004; 2012; Diaz & Puelles 2020). However, we cannot exclude that additional *Tbr1*/TBR1-positive neurons may have migrated tangentially into the EPD locus from the caudally adjoining *prethalamic eminence area*. Such a migration was recently described in chicken embryos on the basis of descriptive developmental *Tbr1* data, subsequently tested experimentally (Alonso et al., 2020, 2021). Note that TBR1 expression also marks glutamatergic, and not GABAergic, neurons in the telencephalon and cerebellum (Hevner et al., 2001, 2006). Consistently with this analysis the EPD does not express any GABAergic markers such as *Gad1* (*Gad67), Slc32a1*, or *Pvalb*/PV (Table 3). Remarkably, all cell populations derived from the prethalamic eminence project to the habenula through the stria medullaris, as occurs with the EPD output.

The EPD population may be partly heterogeneous, since some of its neurons co-express NOS and SST at the dorsal aspect of EPD, whereas the remaining cells express SST but lack NOS signal (Miyamoto and Fukuda 2021; note the neuromorphologic interpretation of these authors followed the columnar model and regarded EPD as a ‘rostral’ subdivision of the entopeduncular nucleus. In any case, the paraventricular area itself is heterogeneous not only rostrocaudally (the EPD being exclusive of the peduncular caudal part) but also dorsoventrally (Puelles & Rubenstein, 2003; Puelles et al., 2012, 2013). It is thus presently unclear whether the EPD origin relates to one or more of the three dorsoventral subdivisions of the peduncular Pa or to the prethalamic eminence (Puelles et al., 2012). We suggest below that the EP_{PEm} formation originates in the dorsalmost Pa portion.

4.3 On the origin of EP_{PRt}

The EP_{PRt} cells are apparently GABAergic; we recently characterized them as being immunoreactive to a pan-DLX antibody but *Dlx5-6-LacZ*-negative (see Figures 2j,k; Puelles

et al. 2021 interpreted this profile as indicative of adult selective expression of Dlx1). These cells share these properties with the prethalamic reticular nucleus, whose neurons express likewise PV/*Pvalb* and SST/*Sst*, and other markers such as *Ecel1*, *Isl1* and *Six3* (Clemence & Mitrofanis, 1992; Puelles et al., 2021; present results). Developmental analysis of *Isl1* expression correlates an early subpial migrating prereticular (PRt) primordium that seems associated to the *Isl*1-positive prethalamic reticular radial domain (present results). These data might support a prethalamic origin of these cells, implying a tangential rostralward migration of alar prethalamic cells into the paraventricular hypothalamic domain, a mechanism which was already suggested previously (Mitrofanis, 1994a,b; Earle & Mitrofanis, 1996; Zhao et al., 2008; Puelles et al., 2012). Indeed, Mitrofanis and collaborators assumed straightforwardly that this entopeduncular population originates jointly with the prethalamic reticular complex. Moreover, Zhao et al. (2008), using a *Foxb1-Cre* mouse line, described a rostralward prethalamic migration of a *Foxb1*-expressing reticular subpopulation that invades the mantle of the peduncular paraventricular region, corroborating Mitrofanisś assumptions.

4.4 On the origin of EP_{PEm}

The prethalamic eminence (PThE) represents within the prosomeric model a hyperdorsal prethalamic progenitor domain placed on top of the central alar prethalamus, wherein the reticular, subgeniculate and pregeniculate nuclei develop. The PThE area is traversed longitudinally by the stria medullaris and limits caudalwards with the thalamic habenular area and rostralwards with the dorsal subdivision of the hypothalamic Pa area, identified recently as the telencephalo-preopto-hypothalamic progenitor domain (POH), characterized differentially by the expression of *Foxg1* from other Pa parts (Morales et al., 2021). The EP_{PEm} population is intercalated between the subpallial substantia innominata domain and the underlying EPD; it was thus judged to occupy a pre-eminential position within the upper part of the Pa area.

4.5 Pallido-entopeduncular homology

Richter (1965), a disciple of H. Spatz (cited above), was the author of an ample monograph on the development of pallidal primordia in primates. He actually provided little substantive data demonstrating a hypothalamic source of the external and internal globus pallidus formations. He rather assumed either migratory or morphogenetic displacement of pallidal primordia supposedly detected first in the hypothalamus into final intratelencephalic positions in primate and human embryos. Richteŕs (1965) delimitations or identifications of the immature early pallidal primordia in his hematoxylin-stained sections seem doubtful in retrospect. This limits the credibility of his schematic reconstructions of the corresponding displacements. Moreover, the sizeable regional morphogenetic deformation patterns he illustrated at the telencephalic stalk, also described by other authors, suggest that there is no real tangential displacement of the pallidal cell masses, as was suggested by Kuhlenbeck (Christ[3] , 1968, footnotes p13, and p20, legend to their Fig.2–6). Moreover, these embryologic interpretations stand in sharp contrast with recent molecular and experimental descriptions of the development of pallidal primordia in mammals or other vertebrates. These systematically provide evidence that the basal ganglia, as a whole, originate and remain within the telencephalic ganglionic eminences (Kodama, 1927; García-López et al.,

2008; Xu et al., 2008; Abellán & Medina, 2009; Flandin et al., 2010; Nóbrega-Pereira et al., 2010; Medina & Abellán 2012; Silberberg et al., 2016). The hypothesis of a diencephalic or hypothalamic origin of pallidal formations (Spatz, 1924, 1925; Richter, 1965; Christ, 1968; Kuhlenbeck, 1973) is rarely if ever mentioned in the molecular era.

In contrast, His (1904) already illustrated distinct proliferative primordia of what was later identified as the medial and lateral ganglionic eminences within the telencephalic vesicle in a 4-month human embryo (see his Fig.61). This alternative and apparently sounder conception was subsequently strongly supported by the technically perfected observations of Hochstetter (1919) and Kodama (1927) on the development of basal ganglia in human embryos. Kodama distinguished medial pallidal from lateral striatal telencephalic mantle primordia at quite early stages (from 2 cm length onwards); it is to be noted that the earliest emerging ganglionic bulge corresponds to the prospective medial ganglionic eminence (including prospective pallidum and diagonal area domains; Puelles et al., 2013, 2016). The rat ganglionic eminences identified by Altman and Bayer (1995) start to become distinguishable at E14 and are essentially identical in topography and aspect with the previously studied human ones. The mouse homologs were visualized molecularly by means of *Nkx2.1* expression starting at E11.5 (Sussel et al., 1999). We thus conclude that there is no significant embryologic support for the notion of a hypothalamic origin of pallidal subpallial primordia.

A different angle for analysis of this issue refers to comparative studies. Modern comparative neuroanatomists that studied striatal and pallidal centers and their connections in non- mammals have uniformly identified homologs of the whole mammalian globus pallidus complex in the telencephalic subpallium, reaching as far back in evolution as agnathans (e.g., Moreno et al., 2009; Stephenson-Jones et al., 2011; Medina et al., 2014); this refers expressly to neurons reported to have mixed external and internal pallidal hodologic properties (Reiner et al., 2004, 2005; Abellán & Medina, 2009; Medina, 2009; Abellán et al., 2010; Kuenzel et al., 2011; Medina & Abellán, 2012; Medina et al., 2014; Suryanarayana et al., 2021; Sugahara et al., 2022). The theory of a hypothalamic/diencephalic origin of pallidal primordia in fact was never extrapolated to non-mammals, as far as we are aware. In no case has evidence of pallidal homologs of any kind been discovered within the hypothalamus in non-mammalian amniotes or anamniotes (Stephenson-Jones et al., 2011; González et al., 2014; Puelles et al., 2013; Grillner & Robertson, 2016; Nieuwenhuys & Puelles, 2016). Puelles et al. (1996) did identify a preincertal entopeduncular nucleus in a frog, whose position suggests homology with our EPV. One or two entopeduncular nuclei also have been postulated tentatively in reptiles and birds (Kuhlenbeck, 1927, 1977; Puelles et al., 2019). Unfortunately, discussion of pallidal homologs in non-mammals has been largely centered in highlighting hodological and chemoarchitectural *similarity*, without systematic consideration of the respective topological positions, developmental origins, and possible migrations (e.g., Puelles & Medina, 2002; Reiner et al., 2004, 2005; but see Puelles et al., 2019).

Our analysis so far thus leads to the conclusion that there exists significant modern evidence (consistent with some earlier embryologic analysis) of various hypothalamic or neighboring prethalamic origins of given mouse entopeduncular formations (at least the four studied

in the present work). These four let's say 'hypothalamic' entities are developmentally independent from the parallel and at least dual telencephalic *pallidal* and *diagonal* ganglionic pallidal anlagen postulated by Puelles et al. (2013), whose partially distinct postnatal and adult molecular profiles apparently contribute to the differential hodological and functional properties of the GPE versus GPI nuclei within basal ganglia circuitry (Figure 10). The different studied molecular and developmental profiles of the four EP populations strongly weigh against the widely assumed homology of a supposedly single 'rodent entopeduncular nucleus' (taken as a whole) with the internal pallidal segment of primates. The remarkable apparent similarities in connectivity and in geno- and chemoarchitecture that do exist between the diagonal MGE-derived GPI, and the subparaventricular hypothalamic EPV component probably have contributed, on top of existing embryologic misinformation, to the prevalent misconception of a homology. The latter hypothesis is supported mainly by circumstantial hodological similarity and somewhat dogmatic transmission in the literature. This conclusion is no longer acceptable after due consideration of the differential embryonic topology of the respective origins of all these cell populations (see homology criteria in Puelles and Medina, 2002; Nieuwenhuys and Puelles 2016). The tentative alternative conclusion that can be derived is that probably most vertebrates possess a homologous bipartite globus pallidus complex in their subpallial telencephalon (see Sadek et al., 2007, for the rat case) and a non-homologous tetrapartite entopeduncular complex in their peduncular hypothalamus.

4. 6 Hodological diversity of EPV and EPD and related homology problems

Although most classic authors reporting connections of rodent EP neurons tended to conceive the population as a single nucleus comparable to the internal segment of the primate globus pallidum, our preliminary efforts to locate the neurons that produce different EP connections are fully consistent with the dual separate EPD/EPV structure described here and elsewhere. Indeed, results weighing in this direction are available from several classic studies (Carter & Fibiger, 1978; Ilinsky & Kultas-Ilinsky, 1987; Heimer et al., 1991, 1995; Herkenham & Nauta, 1977; Nauta, 1974, 1979; A. Parent et al., 1981; M. Parent et al., 1999, 2001; Parent & De Bellefeuille, 1982; van der Kooy & Carter, 1981; Vincent & Brown, 1986).In particular, the study of Miyamoto and Fukuda (2021) recently revealed that EP neurons that project to the lateral habenular nucleus (LHb) lie in our dorsal part of EP (=EPD), are somatostatin- and nitric oxide synthase-positive, and glutamatergic (see also Rajakumar et al., 1993; Vincent & Brown, 1986; Wallace et al., 2017), whereas neurons targeting the motor thalamus seem to lie in our ventral part of EP (= EPV; Kha et al. 2000) and are PV-expressing GABAergic cells (Figure 10b). The glutamatergic EPD cells represent an aversive excitatory habenular connection (Shabel et al., 2012), whereas the EPV projection to the thalamus is inhibitory (Barroso-Chinea et al., 2008; Parent et al., 2001; see Figure 10b). Unfortunately, these studies did not report the potential presence of additional GABAergic neurons retrogradely labeled from the thalamus within what we now define as the telencephalic rodent GPI (diagonal part of MGE), though this point is presently supported by our analysis of experiments illustrated at the Allen Institute for Brain Science (Mouse Brain Connectivity Database).

Interestingly, only the EPV component has a molecular profile resembling that of the diagonal subpallial GPI derivative (both rodent and primate GPI formations originate at this locus, building distinct intermediate mantle strata; Silberberg et al., 2016). The remarkable similarity of GPI and EPV thus extends also to having analogous projections to the motor thalamus, whereas the intercalated EPD clearly projects differentially to the lateral habenula via the stria medullaris (Barroso-Chinea et al., 2008; Fukuda, 2021; Li et al., 2021; Miyamoto & Fukuda (2021); A. Parent et al., 1981; M. Parent et al., 2001; Shabel et al., 2012, 2014; van der Kooy & Carter, 1981; Vincent & Brow, 1986; Wallace et al., 2017).

There is understandably little reference in the literature to telencephalic GPI projections to thalamus in rodents, which would be truly homologous topologically to the thalamic connections coming from the GPI of primates, given that a different homology was widely accepted in most cases. The general expectation was to see motor thalamic projections coming from the spatially distant entopeduncular nucleus, while the actually bipartite rodent globus pallidus complex, assumed to be simply an external globus pallidum homolog was supposed *not to project* to the motor thalamus and to project instead to the subthalamic nucleus (Kim et al., 1976; Nauta & Mehler, 1966). Nevertheless, Nauta (1974, 1979), Severin et al. (1976) and Carter and Fibiger (1978) did report some results suggesting the existence of subpallial globus pallidus projections to the thalamus in the cat and rat, though the latter authors interpreted this result as a possible diffusion artifact, without excluding its possibility. Carter and Fibiger (1978) also reported that retrograde HRP-labeling after experimental injections in the thalamus usually showed labeled neurons in the substantia innominata and the magnocellular preoptic nucleus, which fall within our diagonal developmental territory, that is, the subpallial sector that contains the true (non-entopeduncular) internal globus pallidum (see Puelles et al., 2016).

On the other hand, studies of Parent and collaborators (Parent, 1979, 1986; Parent & De Bellefeuille, 1982; Parent et al., 1984) identified retrogradely the habenulopetal neuronal populations in a monkey. They found what they identified as ‘internal pallidal neurons’ that project to the habenular nuclei. These are largely located *ventromedial* to the thalamopetal neurons found in the primate internal pallidal segment, apparently invading the cerebral peduncle, that is, they have actually an entopeduncular topography, and represent our EPD (Parent et al., 1984; their Fig.1A). Accordingly, we conclude that the topological position of these habenulopetal ‘pallidal’ cells of primates is actually extrapallidal and entopeduncular. This is consistent with hodologically equivalent rodent EPD neurons, as expected comparatively. Primates thus may have an EPD homolog projecting to LHb in a standard paraventricular area-related entopeduncular alar hypothalamic position *outside of the MGE* (see also Hong & Hikosaka, 2008).

We also conclude that both rodents and primates apparently develop primarily a homologous internal globus pallidus component in the inner diagonal part of the MGE. In addition, both primates and rodents probably have a distinct GABAergic EPV component projecting to motor thalamus in their subparaventricular hypothalamus, which has never been searched for as far as we know, but which should be easily localizable in the vecinity of the optic tract with the presently available molecular markers. This structural pattern (possibly complemented with corresponding PE_{PRt} and PE_{PEm} cell groups) may be also demonstrable

generally in other vertebrates, thus significantly enriching our present concept of the basal ganglia complex. The comparative literature frequently mentions that neurons with either GPE or GPI properties are found ‘mixed’ (e.g., Reiner et al., 2004, 2005). While this adult pattern may be a result of either superficial anatomic analysis or postmitotic migrations, our present knowledge on how differential neuronal properties become specified molecularly suggest that separate progenitor domains are probably required, thus implying that more precise developmental and anatomic studies are needed. The GPI apparently does have assorted similarities in molecular and hodological profile with the EPV, but not so the GPE and EPD. However, the GPI and EPV are mutually separated anatomically by the habenulopetal EPD in both rodents and primates, and thus are not the same entities. A differential functional analysis seems required.

Additional more extensive studies on the projections of the rodent true internal globus pallidus compared to the hypothalamic EPV are needed to fully resolve this issue. Such studies should distinguish between the connections of the two telencephalic globus pallidus parts and compare with those of the EPV and EPD.

Our preliminary observations on Allen Mouse Connectivity Data (see Results and Supplementary Figure S1) tend to corroborate our expectations. The mouse GPE projects mainly to the subthalamic nucleus, as well as to both EPD and EPV nuclei, and to the substantia nigra reticulata (similarly as the primate GPE), whereas the mouse GPI projects to the ventral anterior, ventral lateral, and parafascicular thalamic areas, with collaterals to the prethalamic reticular nucleus (similarly as the primate GPI). The subpopulation of cholinergic neurons found within GPI selectively projects to the neocortex in both rodents and primates (Fibiger, 1982; Grove et al., 1986; Ingham et al., 1988, 1985; Mesulam et al., 1983; Saper, 1984). The rodent and primate EPD nucleus selectively projects via the stria medullaris to the lateral habenula (interestingly, the same occurs in zebrafish- Turner et al., 2016- and in a lizard -Diaz & Puelles 1992). We found no Allen experiments centered on the EPV, but corresponding data were reported by Kha et al. (2000), supporting the GABAergic nature of EPV neurons and their targeting of the VA/VL and parafascicular thalamic nuclei, apart a minoritarian cell group that also projected to the lateral habenula (the latter may result from imprecise location of the experiment, possibly involving partially the neighboring EPD).

Given this scenario, we may now attempt to answer tentatively the basic questions: what then is homologous to the rodent EP system in the forebrain of primates? And, where is the real internal globus pallidus homolog in rodents?

As regards the first question, we think the answer is that primates most probably have their own unstudied EP complex with several parts, as found in mice. The general structure of the mammalian brain is extremely conserved and most differences merely relate to quantitative aspects. In this case, the relatively larger size of the cortex of primates leads to a massive difference in size of the peduncular tract compared with that of rodents, so that the diverse entopeduncular populations may be diluted therein and thus be more difficult to recognize anatomically. The group of entopeduncular habenulopetal neurons described by Parent (1986) as a part of the internal pallidum must represent the primate EPD, and

other entopeduncular cells lying more ventrally in the peduncle (roughly at the level of the optic tract) might correspond to EPV. Older published literature is largely unhelpful. However, curiously enough, myelin-stained monkey or human atlas sections often show small unmyelinated islands at the predicted entopeduncular loci inside the peduncle. These islands are sometimes identified globally as the “peduncular comb” and lie roughly alevel with the optic tract (i.e., see Riley, 1943; Mai et al., 1997) and apparently are thought to represent merely packets of unmyelinated fibers that intersect the peduncle. However, there are interstitial neurons accompanying such fibers, as was duly mentioned for the human brain by Alheid et al. (1990; pp 517–520; see their Figures 19.24, 19.25). These authors even identified a chemoarchitectonically distinct posteromedial collection of such neurons as a ‘fourth pallidal division’ which possibly corresponds to the predicted EPV of primates (the internal pallidal segment being subdivided itself into *three* parts; note this allows for additional entopeduncular entities).

Due to the difficulty in localizing the EPV neurons in adult primates (associated with the massive increase in the number of peduncular corticospinal, corticopontine and striatonigral fibers), we presently lack any hodological and little chemoarchitectonic data on them. A number of entopeduncular parvalbumin-positive and calbindin-negative cells were shown by Jones, 1998 (his Figures 24C, D, H, I); these elements might be consistent with the prediction that the primate EPV neurons have thalamopetal projections and are GABAergic, as is the case for their rodent cognates. Reported thalamopetal “perireticular neurons” may correspond also in part to the primate EPV homolog or to the EP_{PRt} (Mitrofanis et al., 1995). Alheid et al. (1990) mentioned that these cells can be distinguished from the remainder of the internal pallidum by an absence of substance P (see also Mai et al., 1986) and by having significant amounts of neurotensin immunoreactivity (Michel et al., 1986).

4.7 Where is the true internal pallidum homolog in rodents?

Congruently with the essentially conserved relative topography and developmental dynamics of most cell populations in the mammalian forebrain, we hypothesize that the two external/internal parts presently distinguished within the rodent globus pallidus (Sadek et al., 2007) represent the rodent external and internal pallidal rudiments, whose cryptic cell-typological differences emerge under genoarchitectonic analysis (present results). In contrast with the extratelencephalic EPD and EPV cell groups, these two pallidal portions develop distinctly inside the telencephalon: the external part in the *pallidal sector* of the medial ganglionic eminence (MGE), and the internal part in the complementary *diagonal sector* (Puelles et al., 2016; Silberberg et al., 2016). The latter corresponds to a subpallial radial histogenetic area found next to the hemispheric stalk, separating the classic pallidal subpallial sector from the preoptic area; it was formerly identified by us as ‘anterior entopeduncular area’ or AEP, a term rooted in Kuhlenbeck’s 1927 early notions (Bulfone et al., 1993; Puelles et al., 2004; Puelles & Rubenstein, 1993, 2003), and was later renamed as ‘diagonal area’, thus referring to a subpial visible classic landmark, the diagonal band (Puelles et al., 2013; 2016).

We first noticed the internal division of the mouse globus pallidus when it was highlighted by the differential way in which *Dlx5/6-LacZ* is expressed in the adjacent pallidal and diagonal MGE sectors, emphasizing cell size differences (differential small versus large

clumps of reaction product appear in the external and internal pallidal parts, respectively; see our Figures 8b–f). Subsequently several other molecular markers (e.g., genes listed in Table 3) were observed to be preferentially expressed in one or the other entity (see also Silberberg et al., 2016 for experimental support).

Supplementary Material

Refer to Web version on PubMed Central for supplementary material.

Acknowledgments:

This work was supported by research grants to CD from Junta de Comunidades de Castilla-La Mancha, SBPLY/21/180501/000047, co-financed by the European Union, and to JLR from NINA IRELAND, NINDS RO1 NS099099, and NIMH R01 MH049428. JLR is cofounder, stockholder, and currently on the scientific board of Neurona, a company studying the potential therapeutic use of interneuron transplantation.

The data that support the findings of this study are available from the corresponding author upon reasonable request.

Abbreviation list

A	amygdala
AA	anterior amygdala
a/b	alar/basal limit
AC	anterior commissural nucleus
ac	anterior commissure
AH	anterior hypothalamic area
AHy	anterior hypophysis
AL	nucleus of the ansa lenticularis
al	ansa lenticularis tract
AV	anteroventral thalamic nucleus
bHL	basal parts of the lateral hypothalamus
BLA	basolateral amygdala
BST	bed nucleus of the stria terminalis
Cb	cerebellum
Ce	central amygdala
CM	central medial thalamic nucleus
Cx	cortex
Dg	diagonal radial domain

DB	diagonal band
EP	entopeduncular nucleus
EPA	accessory entopeduncular nucleus
EPD	dorsal entopeduncular nucleus
EP_{PEm}	entopeduncular preeminential nucleus
EP_{PRt}	entopeduncular prereticular nucleus
EPV	ventral entopeduncular nucleus
F	fornix
Fi	fimbria
GP	globus pallidus
GPE	external globus pallidus
GPI	internal globus pallidus
Hb	habenula
HbL	lateral habenular nucleus
HbM	medial habenular nucleus
HDB	horizontal diagonal band
hdb	hypothalamo-diencephalic boundary
Hi	hippocampal formation
hp1	hypothalamo-telencephalic prosomere 1
hp2	hypothalamo-telencephalic prosomere 2
Hy	hypothalamus
HyB	basal hypothalamus
Ic	internal capsule
Ihv	intrahypothalamic boundary
ivf	interventricular foramen
L	lateral amygdalar nucleus
LGE	lateral ganglionic eminence
LG	lateral geniculate nucleus
Lim	liminar band

LPO	lateral preoptic area
M	mamillary nucleus
MA	medial amygdala
MDL	mediodorsal thalamic nucleus, lateral
MDM	mediodorsal thalamic nucleus, medial
MGE	medial ganglionic eminence
MPO	medial preoptic area
mth	mamillotegmental tract
NLOT	nucleus of the lateral olfactory tract
os	optic stalk
ot	optic tract
p2	prosomere 2
p3	prosomere 3
Pa	paraventricular hypothalamic area
Pal	radial pallidal domain
Pall	pallium
PaV	ventral subregion of the Pa
pe	cerebral peduncle
PF	parafascicular nucleus
PG	prethalamic pregeniculate nucleus
PHy	peduncular hypothalamus
PPa	peduncular paraventricular hypothalamic subdomain
POA	preoptic area
PSPa	peduncular hypothalamic subparaventricular area
PTh	prethalamus
PThE	prethalamic eminence
PThE (vz)	ventricular zone of the PThE
rf	retroflex tract
RLi	rostral liminar band

RM	retromamillary region
Rt	prethalamic reticular nucleus
RTu	retrotuberal hypothalamic region
SCh	suprachiasmatic nucleus
Se	septum
SG	prethalamic subgeniculate nucleus
SI	substantia innominata
SI_{Dg}	diagonal substantia innominata
SI_{Pal}	pallidal substantia innominata
sm	stria medullaris tract
SN	substantia nigra
SNR	reticular substantia nigra
SPa	hypothalamic subparaventricular area
St	striatum
st	stria terminalis
STh	subthalamic nucleus
Th	thalamus
THy	terminal hypothalamus
TPa	terminal paraventricular hypothalamic subdomain
TSPa	terminal subparaventricular hypothalamic subdomain
Tu	olfactory tubercle
TuHy	tuberal hypothalamic region
v	ventricle
VA	ventral anterior thalamic nucleus
VL	ventrolateral thalamic nucleus
VPal	VPall, ventral pallidum
VSt	ventral striatum
vz	ventricular zone
ZI	zona incerta

ZIC	caudal part of the zona incerta
ZIR	rostral part of the zona incerta
zli	zona limitans intrathalamica

References

Abellán A, & Medina L (2009). Subdivisions and derivatives of the chicken subpallium based on expression of LIM and other regulatory genes and markers of neuron subpopulations during development. Journal of Comparative Neurology, 515(4), 465–501. 10.1002/cne.22083 [PubMed: 19459222]

Abellán A, Vernier B, Rétaux S, & Medina L (2010). Similarities and differences in the forebrain expression of Lhx1 and Lhx5 between chicken and mouse: Insights for understanding telencephalic development and evolution. Journal of Comparative Neurology, 518(17), 3512–3528. 10.1002/cne.22410 [PubMed: 20589911]

Acampora D, Postiglione MP, Avantaggiato V, Di Bonito M, Vaccarino FM, Michaud J, & Simeone A (1999). Progressive impairment of developing neuroendocrine cell lineages in the hypothalamus of mice lacking the Orthopedia gene. Genes & Development, 13(21), 2787–2800. 10.1101/gad.13.21.2787

Alheid GF, Heimer L, & Switzer III RC (1990). Basal ganglia. In Paxinos G (Ed.), The Human Nervous System (pp. 483–583). Academic Press.

Alonso A, Trujillo CM, & Puelles L (2020). Longitudinal developmental analysis of prethalamic eminence derivatives in the chick by mapping of Tbr1 in situ expression. Brain Structure and Function, 225(2), 481–510. 10.1007/s00429-019-02015-3 [PubMed: 31901976]

Alonso A, Trujillo CM, & Puelles L (2021). Quail-chick grafting experiments corroborate that Tbr1-positive eminential prethalamic neurons migrate along three streams into hypothalamus, subpallium and septocommissural areas. Brain Structure & Function, 226(3), 759–785. 10.1007/s00429-020-02206-3 [PubMed: 33544184]

Altman J, & Bayer SA (1986). The development of the rat hypothalamus. Advances in Anatomy, Embryology, and Cell Biology, 100, 1–178. [PubMed: 3788679]

Altman J, & Bayer SA (1995). Atlas of Prenatal Rat Brain Development. CRC Press.

Bardet SM, Ferran JLE, Sanchez-Arrones L, & Puelles L (2010). Ontogenetic expression of sonic hedgehog in the chicken subpallium. Frontiers in Neuroanatomy, 4, 28. 10.3389/fnana.2010.00028 [PubMed: 20700498]

Barroso-Chinea P, Rico AJ, Pérez-Manso M, Roda E, López IP, Luis-Ravelo D, & Lanciego JL (2008). Glutamatergic pallidothalamic projections and their implications in the pathophysiology of Parkinson's disease. Neurobiology of Disease, 31(3), 422–432. 10.1016/j.nbd.2008.05.019 [PubMed: 18598767]

Bayer SA (1985). Neurogenesis of the magnocellular basal telencephalic nuclei in the rat. International Journal of Developmental Neuroscience, 3(3), 229–243. 10.1016/0736-5748(85)90028-0 [PubMed: 24874751]

Bulfone A, Puelles L, Porteus MH, Frohman MA, Martin GR, & Rubenstein JL (1993). Spatially restricted expression of Dlx-1, Dlx-2 (Tes-1), Gbx-2, and Wnt-3 in the embryonic day 12.5 mouse forebrain defines potential transverse and longitudinal segmental boundaries. Journal of Neuroscience, 13(7), 3155–3172. 10.1523/JNEUROSCI.13-07-03155.1993 [PubMed: 7687285]

Bulfone A, Smiga SM, Shimamura K, Peterson A, Puelles L, & Rubenstein JL (1995). T-brain-1: A homolog of Brachyury whose expression defines molecularly distinct domains within the cerebral cortex. Neuron, 15(1), 63–78. 10.1016/0896-6273(95)90065-9 [PubMed: 7619531]

Carter DA, & Fibiger HC (1978). The projections of the entopeduncular nucleus and globus pallidus in rat as demonstrated by autoradiography and horseradish peroxidase histochemistry. Journal of Comparative Neurology, 177(1), 113–123. 10.1002/cne.901770108 [PubMed: 411809]

Christ JF (1968). Derivation and boundaries of the hypothalamus, with atlas of hypothalamic grisea. In Anderson E & Nauta WH (Eds.), The Hypothalamus, (pp. 13–60). Charles C. Thomas.

Clemence AE, & Mitrofanis J (1992). Cytoarchitectonic heterogeneities in the thalamic reticular nucleus of cats and ferrets. Journal of Comparative Neurology, 322(2), 167–180. 10.1002/cne.903220203 [PubMed: 1381730]

Cobos I, Puelles L, & Martínez S (2001a). The avian telencephalic subpallium originates inhibitory neurons that invade tangentially the pallium (dorsal ventricular ridge and cortical areas). Developmental Biology, 239(1), 30–45. 10.1006/dbio.2001.0422 [PubMed: 11784017]

Cobos I, Shimamura K, Rubenstein JL, Martínez S, & Puelles L (2001b). Fate map of the avian anterior forebrain at the four-somite stage, based on the analysis of quail-chick chimeras. Developmental Biology, 239(1), 46–67. 10.1006/dbio.2001.0423 [PubMed: 11784018]

Diaz C, de la Torre MM, Rubenstein JLR, & Puelles L (2023). Dorsoventral arrangement of lateral hypothalamus populations in the mouse hypothalamus: A prosomeric genoarchitectonic analysis. Molecular Neurobiology, 60(2), 687–731. 10.1007/s12035-022-03043-7 [PubMed: 36357614]

Diaz C, Morales-Delgado N, & Puelles L (2015). Ontogenesis of peptidergic neurons within the genoarchitectonic map of the mouse hypothalamus. Frontiers in Neuroanatomy, 8, 162. 10.3389/fnana.2014.00162 [PubMed: 25628541]

Diaz C, & Puelles L (1992). Afferent connections of the habenular complex in the lizard Gallotia galloti. Brain, Behavior and Evolution, 39(5), 312–324. 10.1159/000114128 [PubMed: 1498653]

Diaz C, & Puelles L (2020). Developmental genes and malformations in the hypothalamus. Frontiers in Neuroanatomy, 14, 607111. 10.3389/fnana.2020.607111 [PubMed: 33324176]

Diepen R (1962). Nervensystem: Der Hypothalamus. In Möllendorff WV & Bargmann W (Eds.), Handbuch der Mikroskopischen Anatomie des Menschen. IV Band, VII Teil (pp. 1–525). Springer-Verlag

Dudman JT & Gerfen CR (2015). The basal ganglia. Paxinos En G(Ed.), The Rat Nervous System (4th ed., pp. 391–440). Academic Press/Elsevier. 10.1016/B978-0-12-374245-2.00017-6

Earle KL, & Mitrofanis J (1996). Genesis and fate of the perireticular thalamic nucleus during early development. Journal of Comparative Neurology, 367(2), 246–263. 10.1002/(SICI)1096-9861(19960401)367:2<246::AID-CNE7>3.0.CO;2-5 [PubMed: 8708008]

Eid L, & Parent M (2016). Chemical anatomy of pallidal afferents in primates. Brain Structure & Function, 221(9), 4291–4317. 10.1007/s00429-016-1216-y [PubMed: 27028222]

Eisenstat DD, Liu JK, Mione M, Zhong W, Yu G, Anderson SA, Ghattas I, Puelles L, & Rubenstein JL (1999). DLX-1, DLX-2, and DLX-5 expression define distinct stages of basal forebrain differentiation. Journal of Comparative Neurology, 414(2), 217–237. 10.1002/(sici)1096-9861(19991115)414:2<217::aid-cne6>3.0.co;2-i [PubMed: 10516593]

Fan CM, Kuwana E, Bulfone A, Fletcher CF, Copeland NG, Jenkins NA, Crews S, Martinez S, Puelles L, Rubenstein JL, & Tessier-Lavigne M (1996). Expression patterns of two murine homologs of Drosophila single-minded suggest possible roles in embryonic patterning and in the pathogenesis of Down syndrome. Molecular and Cellular Neurosciences, 7(1), 1–16. 10.1006/mcne.1996.0001 [PubMed: 8812055]

Ferran JL, Ayad A-, Mechan P, Morales-Delgado N, Sánchez-Arrones I, & Alonso A (2015). Exploring brain genoarchitecture by single and double chromogenic in situ hybridization (IHS) and immunohistochemistry (IHC) on cryostat, paraffin, or floating sections. In Hauptmann G (Ed.), In situ Hybridization Methods (Vol. 99, pp. 83–107). Springer Science.

Fibiger HC (1982). The organization and some projections of cholinergic neurons of the mammalian forebrain. Brain Research Reviews, 4(3), 327–388. 10.1016/0165-0173(82)90011-X

Flames N, Pla R, Gelman DM, Rubenstein JLR, Puelles L, & Marín O (2007). Delineation of multiple subpallial progenitor domains by the combinatorial expression of transcriptional codes. Journal of Neuroscience, 27(36), 9682–9695. 10.1523/JNEUROSCI.2750-07.2007 [PubMed: 17804629]

Flandin P, Kimura S, & Rubenstein JLR (2010). The progenitor zone of the ventral medial ganglionic eminence requires Nkx2-1 to generate most of the globus pallidus but few neocortical interneurons. Journal of Neuroscience, 30(8), 2812–2823. 10.1523/JNEUROSCI.4228-09.2010 [PubMed: 20181579]

Ganser L (1882). Vergleichend-anatomische Studien über das Gehirn des Maulwurfs. Morphologisches Jahrbuch, 7, 591–725.

García-López M, Abellán A, Legaz I, Rubenstein JLR, Puelles L, & Medina L (2008). Histogenetic compartments of the mouse centromedial and extended amygdala based on gene expression patterns during development. Journal of Comparative Neurology, 506(1), 46–74. 10.1002/cne.21524 [PubMed: 17990271]

Gerfen CR, & Bolam JP (2010). The neuroanatomical organization of the basal ganglia. In Steiner H & Tseng KY (Eds.), Handbook of Behavioral Neuroscience (Vol. 20, pp. 3–28). Elsevier. 10.1016/B978-0-12-374767-9.00001-9

Gerfen CR (2004). Basal ganglia. In Paxinos G(Ed.), The Rat Nervous System (3rd ed., pp. 455–508). Academic Press.

Gilbert MS (1935). The early development of the human diencephalon. Journal of Comparative Neurology, 62(1), 81–115. 10.1002/cne.900620105

González A, Morona R, Moreno N, Bandín S, & López JM (2014). Identification of striatal and pallidal regions in the subpallium of anamniotes. Brain, Behavior and Evolution, 83(2), 93–103. 10.1159/000357754 [PubMed: 24776990]

Gould E, Woolf NJ, & Butcher LL (1991). Postnatal development of cholinergic neurons in the rat: I. Forebrain. Brain Research Bulletin, 27(6), 767–789. 10.1016/0361-9230(91)90209-3 [PubMed: 1664779]

Graybiel AM (1984). Neurochemically specified subsystems in the basal ganglia. Ciba Foundation Symposium, 107, 114–149. 10.1002/9780470720882.ch7 [PubMed: 6149896]

Gribnau AA, & Geijsberts LG (1985). Morphogenesis of the brain in staged rhesus monkey embryos. Advances in Anatomy, Embryology, and Cell Biology, 91, 1–69. 10.1007/978-3-642-69953-5 [PubMed: 3880980]

Grillner S, & Robertson B (2016). The basal ganglia ver 500 million years. Current Biology: CB, 26(20), R1088–R1100. 10.1016/j.cub.2016.06.041 [PubMed: 27780050]

Grove EA, Domesick VB, & Nauta WJ (1986). Light microscopic evidence of striatal input to intrapallidal neurons of cholinergic cell group Ch4 in the rat: A study employing the anterograde tracer Phaseolus vulgaris leucoagglutinin (PHA-L). Brain Research, 367(1–2), 379–384. 10.1016/0006-8993(86)91623-9 [PubMed: 3697714]

Hansen DV, Lui JH, Flandin P, Yoshikawa K, Rubenstein JL, Alvarez-Buylla A, & Kriegstein AR (2013). Non-epithelial stem cells and cortical interneuron production in the human ganglionic eminences. Nature Neuroscience, 16(11), 1576–1587. 10.1038/nn.3541 [PubMed: 24097039]

Hatini V, Tao W, & Lai E (1994). Expression of winged helix genes, BF-1 and BF-2, define adjacent domains within the developing forebrain and retina. Journal of Neurobiology, 25(10), 1293–1309. 10.1002/neu.480251010 [PubMed: 7815060]

Heimer L, de Olmos J, Alheid GF, & Záborszky L (1991). «Perestroika» in the basal forebrain: Opening the border between neurology and psychiatry. Progress in Brain Research, 87, 109–165. 10.1016/s0079-6123(08)63050-2 [PubMed: 1866444]

Heimer L, Zahm DS, & Alheid GF (1995). Basal ganglia. In Paxinos G(Ed.), The Rat Nervous System (2nd ed, pp. 579–628). Academic Press. 10.1046/j.1471-4159.1995.65010471.x

Herkenham M, & Nauta WJ (1977). Afferent connections of the habenular nuclei in the rat. A horseradish peroxidase study, with a note on the fiber-of-passage problem. Journal of Comparative Neurology, 173(1), 123–146. 10.1002/cne.901730107 [PubMed: 845280]

Herrick CJ (1910). The morphology of the forebrain in amphibia and reptilia. Journal of Comparative Neurology and Psychology, 20(5), 413–547. 10.1002/cne.920200502

Hevner RF, Hodge RD, Daza RAM, & Englund C (2006). Transcription factors in glutamatergic neurogenesis: Conserved programs in neocortex, cerebellum, and adult hippocampus. Neuroscience Research, 55(3), 223–233. 10.1016/j.neures.2006.03.004 [PubMed: 16621079]

Hevner RF, Shi L, Justice N, Hsueh Y, Sheng M, Smiga S, Bulfone A, Goffinet AM, Campagnoni AT, & Rubenstein JL (2001). Tbr1 regulates differentiation of the preplate and layer 6. Neuron, 29(2), 353–366. 10.1016/s0896-6273(01)00211-2 [PubMed: 11239428]

His W (1893a). Über das frontale Ende des Gehirnrohrs. Archiv für Anatomie und Entwickelungsgesch [Anatomische Abteilung des Archivs für Anatomie und Physiologie] 3:157–171.

His W (1893b). Vorschläge zur Eintheilung des Gehirns. Archiv für Anatomie und Entwickelungsgesch [Anatomische Abteilung des Archivs für Anatomie und Physiologie 3:172–179.

His W (1904). Die Entwicklung des Menschlichen Gehirns während der Ersten Monate. Hirzel.

Hochstetter F 1929. Beiträge zur Entwicklungsgeschichte des Menschlichen Gehirns. F. Deuticke.

Hong S, & Hikosaka O (2008). The globus pallidus sends reward-related signals to the lateral habenula. Neuron, 60(4), 720–729. 10.1016/j.neuron.2008.09.035 [PubMed: 19038227]

Ilinsky IA, & Kultas-Ilinsky K (1987). Sagittal cytoarchitectonic maps of the Macaca mulatta thalamus with a revised nomenclature of the motor-related nuclei validated by observations on their connectivity. Journal of Comparative Neurology, 262(3), 331–364. 10.1002/cne.902620303 [PubMed: 2821085]

Ingham CA, Bolam JP, & Smith AD (1988). GABA-immunoreactive synaptic boutons in the rat basal forebrain: Comparison of neurons that project to the neocortex with pallidosubthalamic neurons. Journal of Comparative Neurology, 273(2), 263–282. 10.1002/cne.902730210 [PubMed: 3417904]

Ingham CA, Bolam JP, Wainer BH, & Smith AD (1985). A correlated light and electron microscopic study of identified cholinergic basal forebrain neurons that project to the cortex in the rat. Journal of Comparative Neurology, 239(2), 176–192. 10.1002/cne.902390205 [PubMed: 4044933]

Jiao Y, Medina L, Veenman CL, Toledo C, Puelles L, & Reiner A (2000). Identification of the anterior nucleus of the ansa lenticularis in birds as the homolog of the mammalian subthalamic nucleus. Journal of Neuroscience, 20(18), 6998–7010. 10.1523/jneurosci.20-18-06998.2000 [PubMed: 10995845]

Jones EG (1998). Viewpoint: The core and matrix of thalamic organization. Neuroscience, 85(2), 331–345. 10.1016/s0306-4522(97)00581-2 [PubMed: 9622234]

Kahle W (1956). Zur Entwicklung des menschlichen Zwischenhirnes. Deutsche Zeitschrift für Nervenheilkunde, 175(3), 259–318. 10.1007/BF00242726 [PubMed: 13397345]

Kahle W (1969). Die Entwicklung der menschlichen Grosshirnhemisphäre. In Neurology Series (Vol. 1). Springer.

Kappers CUA (1921). Die vergleichende Anatomie des Nervensystems der Wirbeltiere und des Menschen (Vol. 2). Bohn.

Keyser A (1972). The development of the diencephalon of the Chinese hamster. Acta Morphologica Neerlando-Scandinavica, 9(4), 379. [PubMed: 5055997]

Keyser A (1979). Development of the hypothalamus in mammals. An investigation into its morphological position during ontogenesis. In Morgane PJ & Panksepp J (Eds.), Handbook of the Hypothalamus (Vol. 1, pp. 65–136). Marcel.

Kha HT, Finkelstein DI, Pow DV, Lawrence AJ, & Horne MK (2000). Study of projections from the entopeduncular nucleus to the thalamus of the rat. Journal of Comparative Neurology, 426(3), 366–377. [PubMed: 10992243]

Kim DW, Liu K, Wang ZQ, Zhang YS, Bathini A, Brown MP, Lin SH, Washington PW, Sun C, Lindtner S, Lee B, Wang H, Shimogori T, Rubenstein JLR, & Blackshaw S (2021). Gene regulatory networks controlling differentiation, survival, and diversification of hypothalamic Lhx6-expressing GABAergic neurons. Communications Biology, 4(1), 95. 10.1038/s42003-020-01616-7 [PubMed: 33479483]

Kim R, Nakano K, Jayaraman A, & Carpenter MB (1976). Projections of the globus pallidus and adjacent structures: An autoradiographic study in the monkey. Journal of Comparative Neurology, 169(3), 263–290. 10.1002/cne.901690302 [PubMed: 823180]

Kimura S, Hara Y, Pineau T, Fernandez-Salguero P, Fox CH, Ward JM, & Gonzalez FJ (1996). The T/ebp null mouse: Thyroid-specific enhancer-binding protein is essential for the organogenesis of the thyroid, lung, ventral forebrain, and pituitary. Genes & Development, 10(1), 60–69. 10.1101/gad.10.1.60 [PubMed: 8557195]

Kodama S (1927). Über die Entwicklung des striären Systems beim Menschen. In Neurologische und Psychiatrische Abhandlungen aus der Schweiz. Archiv für Neurologie und Psychiatrie, Heft 5 (pp. 1–98). Orell Füssli Verlag.

Kuenzel WJ, Medina L, Csillag A, Perkel DJ, & Reiner A (2011). The avian subpallium: New insights into structural and functional subdivisions occupying the lateral subpallial wall and their

embryological origins. Brain Research, 1424, 67–101. 10.1016/j.brainres.2011.09.037 [PubMed: 22015350]

Kuhlenbeck H (1924). Über die Homologien der Zellmassen im Hemispherenhirn der Wirbeltiere. Folia Anatomica. Japonica, 2, 325–364.

Kuhlenbeck H (1927). Vorlesungen über das Zentralnervensystem der Wirbeltiere: eine Einführung in die Gehirnanatomie auf vergleichender Grundlage. Gustav Fischer.

Kuhlenbeck H (1954). The human diencephalon; a summary of development, structure, function, and pathology. Confinia Neurologica, 14, 1–230.

Kuhlenbeck H (1973). The Central Nervous System of Vertebrates. Vol.3, part II: Overall Morphological Pattern. Karger.

Kuhlenbeck H (1977). Central Nervous System of Vertebrates. Vol.5, part I: Derivatives of the Prosencephalon: Diencephalon and Telencephalon. Karger.

Kuhlenbeck H, & Haymaker W (1949). The derivatives of the hypothalamus in the human brain; their relation to the extrapyramidal and autonomic systems. Military Surgeon, 105(1), 26–52. 10.1093/milmed/105.1.26 [PubMed: 18135373]

Lavdas AA, Grigoriou M, Pachnis V, & Parnavelas JG (1999). The medial ganglionic eminence gives rise to a population of early neurons in the developing cerebral cortex. Journal of Neuroscience, 19(18), 7881–7888. 10.1523/JNEUROSCI.19-18-07881.1999 [PubMed: 10479690]

Li H, Eid M, Pullmann D, Chao YS, Thomas AA, & Jhou TC (2021). Entopeduncular nucleus projections to the lateral habenula contribute to cocaine avoidance. Journal of Neuroscience, 41(2), 298–306. 10.1523/JNEUROSCI.0708-20.2020 [PubMed: 33214316]

Li Y, Holtzman DM, Kromer LF, Kaplan DR, Chua-Couzens J, Clary DO, Knusel B, & Mobley WC (1995). Regulation of TrkA and ChAT expression in developing rat basal forebrain: Evidence that both exogenous and endogenous NGF regulate differentiation of cholinergic neurons. Journal of Neuroscience, 15(4), 2888–2905. 10.1523/JNEUROSCI.15-04-02888.1995 [PubMed: 7536822]

Liu JK, Ghattas I, Liu S, Chen S, & Rubenstein JL (1997). Dlx genes encode DNA-binding proteins that are expressed in an overlapping and sequential pattern during basal ganglia differentiation. Developmental Dynamics, 210(4), 498–512. 10.1002/(SICI)1097-0177(199712)210:4<498::AID-AJA12>3.0.CO;2-3 [PubMed: 9415433]

Long JE, Swan C, Liang WS, Cobos I, Potter GB, & Rubenstein JLR (2009). Dlx1&2 and Mash1 transcription factors control striatal patterning and differentiation through parallel and overlapping pathways. Journal of Comparative Neurology, 512(4), 556–572. 10.1002/cne.21854 [PubMed: 19030180]

Loo YT (1931). The forebrain of the opossum Didelphis virginiana. Part II. Histology. Journal of Comparative Neurology 52, 1–148. 10.1002/cne.900520102

López-González L, Alonso A, García-Calero E, de Puelles E, & Puelles L (2021). Tangential intrahypothalamic migration of the mouse ventral premamillary nucleus and Fgf8 signaling. Frontiers in Cell and Developmental Biology, 9, 676121. 10.3389/fcell.2021.676121 [PubMed: 34095148]

Ma T, Wang C, Wang L, Zhou X, Tian M, Zhang Q, Zhang Y, Li J, Liu Z, Cai Y, Liu F, You Y, Chen C, Campbell K, Song H, Ma L, Rubenstein JL, & Yang Z (2013). Subcortical origins of human and monkey neocortical interneurons. Nature Neuroscience, 16(11), 1588–1597. 10.1038/nn.3536 [PubMed: 24097041]

Mai JK, Stephens PH, Hopf A, & Cuello AC (1986). Substance P in the human brain. Neuroscience, 17(3), 709–739. 10.1016/0306-4522(86)90041-2 [PubMed: 2422595]

Mai JK, Assheuer J, & Paxinos G (1997). Atlas of the Human Brain. Academic Press.

Marchand R, & Poirier LJ (1983). Isthmic origin of neurons of the rat substantia nigra. Neuroscience, 9(2), 373–381. 10.1016/0306-4522(83)90300-7 [PubMed: 6877599]

Marchand R, Lajoie L, & Blanchet C (1986). Histogenesis at the level of the basal forebrain: The entopeduncular nucleus. Neuroscience, 17(3), 591–607. 10.1016/0306-4522(86)90032-1 [PubMed: 3703250]

Marin O, Anderson SA, & Rubenstein JL (2000). Origin and molecular specification of striatal interneurons. Journal of Neuroscience, 20(16), 6063–6076. [PubMed: 10934256]

Marín O, Baker J, Puelles L, & Rubenstein JLR (2002). Patterning of the basal telencephalon and hypothalamus is essential for guidance of cortical projections. Development, 129(3), 761–773. 10.1242/dev.129.3.761 [PubMed: 11830575]

Marín O, González A, & Smeets WJ (1997). Basal ganglia organization in amphibians: Afferent connections to the striatum and the nucleus accumbens. Journal of Comparative Neurology, 378(1), 16–49. 10.1002/(sici)1096-9861(19970203)378:1<16::aid-cne2>3.0.co;2-n [PubMed: 9120053]

Martin DM, Probst FJ, Fox SE, Schimmenti LA, Semina EV, Hefner MA, Belmont JW, & Camper SA (2002). Exclusion of PITX2 mutations as a major cause of CHARGE association. American Journal of Medical Genetics, 111(1), 27–30. 10.1002/ajmg.10473 [PubMed: 12124729]

Martin DM, Skidmore JM, Philips ST, Vieira C, Gage PJ, Condie BG, Raphael Y, Martinez S, & Camper SA (2004). PITX2 is required for normal development of neurons in the mouse subthalamic nucleus and midbrain. Developmental Biology, 267(1), 93–108. 10.1016/j.ydbio.2003.10.035 [PubMed: 14975719]

Martínez S, & Puelles L (2000). Neurogenetic compartments of the mouse diencephalon and some characteristic gene expression patterns. Results and Problems in Cell Differentiation, 30, 91–106. 10.1007/978-3-540-48002-0_4 [PubMed: 10857186]

Martínez-de-la-Torre M, Pombal MA, & Puelles L (2011). Distal-less-like protein distribution in the larval lamprey forebrain. Neuroscience, 178, 270–284. 10.1016/j.neuroscience.2010.12.030 [PubMed: 21185911]

Martinez-Garcia F, Novejarque A, & Lanuza E (2007). Evolution of the amygdala in vertebrates. In Kaas JH & Bullok TH (Eds.), Evolution of Nervous Systems. A Comprehensive Reference (pp. 255–334). Academic Press/Elsevier. 10.1016/B0-12-370878-8/00139-7

Medina L (2007). 1.05—Field homologies. Kaas En J. H. (Ed.), Evolution of Nervous Systems (pp. 73–87). Academic Press. 10.1016/B0-12-370878-8/00097-5

Medina L (2009). Basal Ganglia: Evolution. In Squire LR(Ed.), Encyclopedia of Neuroscience (pp. 67–85). Academic Press. 10.1016/B978-008045046-9.00933-5

Medina L, & Abellán A (2012). Subpallial structures. In Watson C, Paxinos G, & Puelles L (Eds.), The Mouse Nervous System (pp. 173–220). Academic Press. 10.1016/B978-0-12-369497-3.10007-X

Medina L, Abellán A, Vicario A, & Desfilis E (2014). Evolutionary and developmental contributions for understanding the organization of the basal ganglia. Brain, Behavior and Evolution, 83(2), 112–125. 10.1159/000357832 [PubMed: 24776992]

Medina L, Brox A, Legaz I, García-López M, & Puelles L (2005). Expression patterns of developmental regulatory genes show comparable divisions in the telencephalon of Xenopus and mouse: Insights into the evolution of the forebrain. Brain Research Bulletin, 66(4–6), 297–302. 10.1016/j.brainresbull.2005.02.003 [PubMed: 16144605]

Mesulam MM, Mufson EJ, Levey AI, & Wainer BH (1983). Cholinergic innervation of cortex by the basal forebrain: Cytochemistry and cortical connections of the septal area, diagonal band nuclei, nucleus basalis (substantia innominata), and hypothalamus in the rhesus monkey. Journal of Comparative Neurology, 214(2), 170–197. 10.1002/cne.902140206 [PubMed: 6841683]

Métin C, Alvarez C, Moudoux D, Vitalis T, Pieau C, & Molnár Z (2007). Conserved pattern of tangential neuronal migration during forebrain development. Development, 134(15), 2815–2827. 10.1242/dev.02869 [PubMed: 17611228]

Michel JP, Sakamoto N, Kopp N, & Pearson J (1986). Neurotensin immunoreactive structures in the human infant striatum, septum, amygdala and cerebral cortex. Brain Research, 397(1), 93–102. 10.1016/0006-8993(86)91372-7 [PubMed: 3542118]

Mitrofanis J (1992). Patterns of antigenic expression in the thalamic reticular nucleus of developing rats. Journal of Comparative Neurology, 320(2), 161–181. 10.1002/cne.903200203 [PubMed: 1377717]

Mitrofanis J (1994a). Development of the pathway from the reticular and perireticular nuclei to the thalamus in ferrets: a Dil study. European Journal of Neuroscience, 6(12), 1864–1882. 10.1111/j.1460-9568.1994.tb00578.x [PubMed: 7704297]

Mitrofanis J (1994b). Development of the thalamic reticular nucleus in ferrets with special reference to the perigeniculate and perireticular cell groups. European Journal of Neuroscience, 6(2), 253–263. 10.1111/j.1460-9568.1994.tb00268.x [PubMed: 7513240]

Mitrofanis J, & Baker GE (1993). Development of the thalamic reticular and perireticular nuclei in rats and their relationship to the course of growing corticofugal and corticopetal axons. Journal of Comparative Neurology, 338(4), 575–587. 10.1002/cne.903380407 [PubMed: 8132862]

Mitrofanis J, Lozsádi DA, & Coleman KA (1995). Evidence for a projection from the perireticular thalamic nucleus to the dorsal thalamus in the adult rat and ferret. Journal of Neurocytology, 24(12), 891–902. 10.1007/BF01215640 [PubMed: 8719817]

Miyamoto Y, & Fukuda T (2015). Immunohistochemical study on the neuronal diversity and three-dimensional organization of the mouse entopeduncular nucleus. Neuroscience Research, 94, 37–49. 10.1016/j.neures.2015.02.006 [PubMed: 25722090]

Miyamoto Y, & Fukuda T (2021). The habenula-targeting neurons in the mouse entopeduncular nucleus contain not only somatostatin-positive neurons but also nitric oxide synthase-positive neurons. Brain Structure & Function, 226(5), 1497–1510. 10.1007/s00429-021-02264-1 [PubMed: 33787995]

Morales L, Castro-Robles B, Abellán A, Desfilis E, & Medina L (2021). A novel telencephalon-opto-hypothalamic morphogenetic domain coexpressing Foxg1 and Otp produces most of the glutamatergic neurons of the medial extended amygdala. Journal of Comparative Neurology, 529(10), 2418–2449. 10.1002/cne.25103 [PubMed: 33386618]

Morales-Delgado N, Castro-Robles B, Ferrán JL, Martinez-de-la-Torre M, Puelles L, & Díaz C (2014). Regionalized differentiation of CRH, TRH, and GHRH peptidergic neurons in the mouse hypothalamus. Brain Structure & Function, 219(3), 1083. 10.1007/s00429-013-0554-2 [PubMed: 24337236]

Morales-Delgado N, Merchan P, Bardet SM, Ferrán JL, Puelles L, & Díaz C (2011). Topography of somatostatin gene expression relative to molecular progenitor domains during ontogeny of the mouse hypothalamus. Frontiers in Neuroanatomy, 5. 10.3389/fnana.2011.00010

Moreno N, Domínguez L, Rétaux S, & González A (2008a). Islet1 as a marker of subdivisions and cell types in the developing forebrain of Xenopus. Neuroscience, 154(4), 1423–1439. 10.1016/j.neuroscience.2008.04.029 [PubMed: 18515014]

Moreno N, González A, & Rétaux S (2008b). Evidences for tangential migrations in Xenopus telencephalon: Developmental patterns and cell tracking experiments. Developmental Neurobiology, 68(4), 504–520. 10.1002/dneu.20603 [PubMed: 18214835]

Moreno N, González A, & Rétaux S (2009). Development and evolution of the subpallium. Seminars in Cell & Developmental Biology, 20(6), 735–743. 10.1016/j.semcdb.2009.04.007 [PubMed: 19374952]

Moreno N, López JM, Morona R, Lozano D, Jiménez S, & González A (2018). Comparative analysis of Nkx2.1 and Islet-1 expression in urodele amphibians and lungfishes highlights the pattern of forebrain organization in early tetrapods. Frontiers in Neuroanatomy, 12, 42. 10.3389/fnana.2018.00042 [PubMed: 29867380]

Moreno N, Morona R, López JM, & González A (2010). Subdivisions of the turtle Pseudemys scripta subpallium based on the expression of regulatory genes and neuronal markers. Journal of Comparative Neurology, 518(24), 4877–4902. 10.1002/cne.22493 [PubMed: 21031557]

Moreno N, Rétaux S, & González A (2008c). Spatio-temporal expression of Pax6 in Xenopus forebrain. Brain Research, 1239, 92–99. 10.1016/j.brainres.2008.08.052 [PubMed: 18786519]

Nauta HJ (1974). Evidence of a pallidohabenular pathway in the cat. Journal of Comparative Neurology, 156(1), 19–27. 10.1002/cne.901560103 [PubMed: 4857835]

Nauta HJ (1979). Projections of the pallidal complex: An autoradiographic study in the cat. Neuroscience, 4(12), 1853–1873. 10.1016/0306-4522(79)90060-5 [PubMed: 530436]

Nauta WJ, & Mehler WR (1966). Projections of the lentiform nucleus in the monkey. Brain Research, 1(1), 3–42. 10.1016/0006-8993(66)90103-x [PubMed: 4956247]

Ni R-J, Huang Z-H, Shu Y-M, Wang Y, Li T, & Zhou J-N (2018). Atlas of the striatum and globus pallidus in the tree shrew: Comparison with rat and mouse. Neuroscience Bulletin, 34(3), 405–418. 10.1007/s12264-018-0212-z [PubMed: 29508249]

Nieuwenhuys R & Puelles L (2016). Towards a new Neuromorphology. Springer. 10.1007/978-3-319-25693-1

Nieuwenhuys R, Voogd J, & van Huijzen C (2008). The Human Central Nervous System (4th ed.). Springer-Verlag. 10.1007/978-3-540-34686-9

Nóbrega-Pereira S, Gelman D, Bartolini G, Pla R, Pierani A, & Marín O (2010). Origin and molecular specification of globus pallidus neurons. Journal of Neuroscience, 30(8), 2824–2834. 10.1523/JNEUROSCI.4023-09.2010 [PubMed: 20181580]

Oh JD, Woolf NJ, Roghani A, Edwards RH, & Butcher LL (1992). Cholinergic neurons in the rat central nervous system demonstrated by in situ hybridization of choline acetyltransferase mRNA. Neuroscience, 47(4), 807–822. 10.1016/0306-4522(92)90031-v [PubMed: 1579211]

Oorschot DE (2016). Cell types in the different nuclei of the basal ganglia. In Steiner H & Tseng KY (Eds.), Handbook of Behavioral Neuroscience (Vol. 24, pp. 99–117). Elsevier. 10.1016/B978-0-12-802206-1.00005-2

Papez JW (1940). The embryologic development of the hypothalamic area in mammals. In Haynaker W, Anderson E, Nauta WH (Eds), The Hypothalamus. Charles C. Thomas.

Parent A (1979). Identification of the pallidal and peripallidal cells projecting to the habenula in monkey. Neuroscience Letters, 15(2–3), 159–164. 10.1016/0304-3940(79)96106-8 [PubMed: 119192]

Parent A (1986). Comparative Neurobiology of the Basal Ganglia. Wiley.

Parent A, Bouchard C, & Smith Y (1984). The striatopallidal and striatonigral projections: Two distinct fiber systems in primate. Brain Research, 303(2), 385–390. 10.1016/0006-8993(84)91224-1 [PubMed: 6744030]

Parent A, & De Bellefeuille L (1982). Organization of efferent projections from the internal segment of globus pallidus in primate as revealed by fluorescence retrograde labeling method. Brain Research, 245(2), 201–213. 10.1016/0006-8993(82)90802-2 [PubMed: 7127069]

Parent A, De Bellefeuille L, & Mackey A (1984). Organization of primate internal pallidum as revealed by fluorescent retrograde tracing of its efferent projections. In Hassler RG & Christ JF (Eds.), Advances in Neurology (Vol. 40, pp. 15–20). Raven Press. [PubMed: 6421108]

Parent A, Gravel S, & Boucher R (1981). The origin of forebrain afferents to the habenula in rat, cat and monkey. Brain Research Bulletin, 6(1), 23–38. 10.1016/s0361-9230(81)80066-4 [PubMed: 7470948]

Parent A, & Hazrati LN (1995a). Functional anatomy of the basal ganglia. I. The cortico-basal ganglia-thalamo-cortical loop. Brain Research. Brain Research Reviews, 20(1), 91–127. 10.1016/0165-0173(94)00007-c [PubMed: 7711769]

Parent A, & Hazrati LN (1995b). Functional anatomy of the basal ganglia. II. The place of subthalamic nucleus and external pallidum in basal ganglia circuitry. Brain Research. Brain Research Reviews, 20(1), 128–154. 10.1016/0165-0173(94)00008-d [PubMed: 7711765]

Parent M, Lévesque M, & Parent A (1999). The pallidofugal projection system in primates: Evidence for neurons branching ipsilaterally and contralaterally to the thalamus and brainstem. Journal of Chemical Neuroanatomy, 16(3), 153–165. 10.1016/s0891-0618(99)00008-3 [PubMed: 10422736]

Parent M, Lévesque M, & Parent A (2001). Two types of projection neurons in the internal pallidum of primates: Single-axon tracing and three-dimensional reconstruction. Journal of Comparative Neurology, 439(2), 162–175. 10.1002/cne.1340 [PubMed: 11596046]

Pauly M-C, Döbrössy MD, Nikkhah G, Winkler C, & Piroth T (2013). Organization of the human fetal subpallium. Frontiers in Neuroanatomy, 7, 54. 10.3389/fnana.2013.00054 [PubMed: 24474906]

Paxinos G, & Watson C (2014). The Rat Brain in Stereotaxic Coordinates (7th ed.). Elsevier Academic Press.

Percheron G, Francois C, Yelnik J, Fenelon G, & Talbi B (1994). The basal ganglia related system of primates: Definition, description and informational analysis. In Percheron G, McKenzie JS, & Féger J (Eds.), The Basal Ganglia IV. New Ideas and Data on Structure and Function (pp. 3–20). Plenum Press. 10.1007/978-1-4613-0485-2

Pombal MA, Megías M, Bardet SM, & Puelles L (2009). New and old thoughts on the segmental organization of the forebrain in lampreys. Brain, Behavior and Evolution, 74(1), 7–19. 10.1159/000229009 [PubMed: 19729892]

Posch DK, Schwabe K, Krauss JK, & Lütjens G (2012). Deep brain stimulation of the entopeduncular nucleus in rats prevents apomorphine-induced deficient sensorimotor gating. Behavioural Brain Research, 232(1), 130–136. 10.1016/j.bbr.2012.02.046 [PubMed: 22425742]

Puelles L (2017). Forebrain development in vertebrates. The evolutionary role of secondary organizers. In Shepherd S,V(Ed.), The Wiley Handbook of Evolutionary Neuroscience, (pp. 350–387). John Wiley & Sons. 10.1002/9781118316757.ch12

Puelles L (2018). Developmental studies of avian brain organization. The International Journal of Developmental Biology, 62(1-2-3), 207–224. 10.1387/ijdb.170279LP. [PubMed: 29616730]

Puelles L (2022). Current status of the hypothesis of a claustro-insular homolog in sauropsids. Brain, Behavior and Evolution, 96(4–6), 212–241. 10.1159/000520742 [PubMed: 34753135]

Puelles L, Alonso A, García-Calero E, & Martínez-de-la-Torre M. (2019). Concentric ring topology of mammalian cortical sectors and relevance for patterning studies. Journal of Comparative Neurology, 527(10), 1731–1752. 10.1002/cne.24650. [PubMed: 30737959]

Puelles L, Diaz C, Stühmer T, Ferran JL, Martínez-de la Torre M, & Rubenstein JLR (2021). LacZ-reporter mapping of Dlx5/6 expression and genoarchitectural analysis of the postnatal mouse prethalamus. Journal of Comparative Neurology, 529(2), 367–420. 10.1002/cne.24952 [PubMed: 32420617]

Puelles L, Harrison M, Paxinos G, & Watson C (2013). A developmental ontology for the mammalian brain based on the prosomeric model. Trends in Neurosciences, 36(10), 570–578. 10.1016/j.tins.2013.06.004 [PubMed: 23871546]

Puelles L, Javier Milán F, & Martínez-de-la-Torre M (1996). A segmental map of architectonic subdivisions in the diencephalon of the frog Rana perezi: Acetylcholinesterase-histochemical observations. Brain, Behavior and Evolution, 47(6), 279–310. 10.1159/000113247 [PubMed: 8796963]

Puelles L, Kuwana E, Puelles E, Bulfone A, Shimamura K, Keleher J, Smiga S, & Rubenstein JL (2000). Pallial and subpallial derivatives in the embryonic chick and mouse telencephalon, traced by the expression of the genes Dlx-2, Emx-1, Nkx-2.1, Pax-6, and Tbr-1. Journal of Comparative Neurology, 424(3), 409–438. 10.1002/1096-9861(20000828)424:3<409::aid-cne3>3.0.co;2-7 [PubMed: 10906711]

Puelles L, Martínez S, Martínez-de-la-Torre M, & Rubenstein JLR (2004). Gene maps and related histogenetic domains in the forebrain and midbrain. In Paxinos G(Ed.), The Rat Nervous System (pp. 3–25). Academic Press/Elsevier.

Puelles L, Martinez-de-la-Torre M, Bardet SM, & Rubenstein JLR (2012). Hypothalamus. In Watson C, Paxinos G, & Puelles L (Eds.), The Mouse Nervous System. (pp. 221–312). Academic Press/Elsevier.

Puelles L, Martinez-de-la-Torre M, Martínez S, Watson C, & Paxinos G (2019). The Chick Brain in Stereotaxic Coordinates and Alternate Stains (2nd ed.). Academic Press/Elsevier.

Puelles L, & Medina L (2002). Field homology as a way to reconcile genetic and developmental variability with adult homology. Brain Research Bulletin, 57(3–4), 243–255. 10.1016/s0361-9230(01)00693-1 [PubMed: 11922968]

Puelles L, Morales-Delgado N, Merchán P, Castro-Robles B, Martínez-de-la-Torre M, Díaz C, & Ferran JL (2016). Radial and tangential migration of telencephalic somatostatin neurons originated from the mouse diagonal area. Brain Structure & Function, 221(6), 3027–3065. 10.1007/s00429-015-1086-8

Puelles L, & Rubenstein JL (1993). Expression patterns of homeobox and other putative regulatory genes in the embryonic mouse forebrain suggest a neuromeric organization. Trends in Neurosciences, 16(11), 472–479. 10.1016/0166-2236(93)90080-6 [PubMed: 7507621]

Puelles L, & Rubenstein JLR (2003). Forebrain gene expression domains and the evolving prosomeric model. Trends in Neurosciences, 26(9), 469–476. 10.1016/S0166-2236(03)00234-0 [PubMed: 12948657]

Puelles L, & Rubenstein JLR (2015). A new scenario of hypothalamic organization: Rationale of new hypotheses introduced in the updated prosomeric model. Frontiers in Neuroanatomy, 9, 27. 10.3389/fnana.2015.00027 [PubMed: 25852489]

Rajakumar N, Elisevich K, & Flumerfelt BA (1993). Compartmental origin of the striato-entopeduncular projection in the rat. Journal of Comparative Neurology, 331(2), 286–296. 10.1002/cne.903310210 [PubMed: 8509503]

Ramón y Cajal S (1903). Estudios talámicos. Trabajos de laboratorio de Investigaciones Biológicas, 2, 31–69.

Reiner A (2016). The conservative evolution of the vertebrate basal ganglia. In Steiner H & Tseng KY (Eds.), Handbook of Behavioral Neuroscience (Vol. 24, pp. 63–97). Elsevier. 10.1016/B978-0-12-802206-1.00004-0

Reiner A, Medina L, & Veenman CL (1998). Structural and functional evolution of the basal ganglia in vertebrates. Brain Research. Brain Research Reviews, 28(3), 235–285. 10.1016/s0165-0173(98)00016-2 [PubMed: 9858740]

Reiner A, Perkel DJ, Bruce LL, Butler AB, Csillag A, Kuenzel W, Medina L, Paxinos G, Shimizu T, Striedter G, Wild M, Ball GF, Durand S, Gütürkün O, Lee DW, Mello CV, Powers A, White SA, Hough G, … Jarvis ED (2004). The avian brain nomenclature forum: terminology for a new century in comparative neuroanatomy. Journal of Comparative Neurology, 473, E1–E6. 10.1002/cne.20119 [PubMed: 19626136]

Reiner A, Yamamoto K, & Karten HJ (2005). Organization and evolution of the avian forebrain. The Anatomical Record Part A, Discoveries in Molecular, Cellular, and Evolutionary Biology, 287(1), 1080–1102. 10.1002/ar.a.20253 [PubMed: 16206213]

Richter E (1965). Die Entwicklung des Globus Pallidus und des Corpus Subthalamicum (Vol. 108). Springer Berlin.

Riley HA (1943). An Atlas of the Basal Ganglia, Brain Stem, and Spinal Cord. Hafner Publishing Company.

Rose JE (1942). The ontogenetic development of the rabbit's diencephalon. Journal of Comparative Neurology, 77(1), 61–129. 10.1002/cne.900770105

Rubenstein JL, Martinez S, Shimamura K, & Puelles L (1994). The embryonic vertebrate forebrain: The prosomeric model. Science, 266(5185), 578–580. 10.1126/science.7939711 [PubMed: 7939711]

Sadek AR, Magill PJ, & Bolam JP (2007). A single-cell analysis of intrinsic connectivity in the rat globus pallidus. Journal of Neuroscience, 27(24), 6352–6362. 10.1523/JNEUROSCI.0953-07.2007 [PubMed: 17567796]

Saper CB (1984). Organization of cerebral cortical afferent systems in the rat. II. Magnocellular basal nucleus. Journal of Comparative Neurology, 222(3), 313–342. 10.1002/cne.902220302 [PubMed: 6699210]

Severin CM, Young PA, & Massapust LC (1976). Pallidothalamic projections in the rat. Journal of Comparative Neurology, 166(4), 491–502. 10.1002/cne.901660409 [PubMed: 1270619]

Shabel SJ, Proulx CD, Piriz J, & Malinow R (2014). Mood regulation. GABA/glutamate co-release controls habenula output and is modified by antidepressant treatment. Science, 345(6203), 1494–1498. 10.1126/science.1250469 [PubMed: 25237099]

Shabel SJ, Proulx CD, Trias A, Murphy RT, & Malinow R (2012). Input to the lateral habenula from the basal ganglia is excitatory, aversive, and suppressed by serotonin. Neuron, 74(3), 475–481. 10.1016/j.neuron.2012.02.037 [PubMed: 22578499]

Shimamura K, Martinez S, Puelles L, & Rubenstein JL (1997). Patterns of gene expression in the neural plate and neural tube subdivide the embryonic forebrain into transverse and longitudinal domains. Developmental Neuroscience, 19(1), 88–96. 10.1159/000111190 [PubMed: 9078438]

Shimogori T, Lee DA, Miranda-Angulo A, Yang Y, Wang H, Jiang L, Yoshida AC, Kataoka A, Mashiko H, Avetisyan M, Qi L, Qian J, & Blackshaw S (2010). A genomic atlas of mouse hypothalamic development. Nature Neuroscience, 13(6), 767–775. 10.1038/nn.2545 [PubMed: 20436479]

Sidman RL, & Rakic P (1973). Neuronal migration, with special reference to developing human brain: A review. Brain Research, 62(1), 1–35. 10.1016/0006-8993(73)90617-3 [PubMed: 4203033]

Silberberg SN, Taher L, Lindtner S, Sandberg M, Nord AS, Vogt D, Mckinsey GL, Hoch R, Pattabiraman K, Zhang D, Ferran JL, Rajkovic A, Golonzhka O, Kim C, Zeng H, Puelles L, Visel A, & Rubenstein JLR (2016). Subpallial enhancer transgenic lines: A data and tool resource to study transcriptional regulation of GABAergic cell fate. Neuron, 92(1), 59–74. 10.1016/j.neuron.2016.09.027 [PubMed: 27710791]

Simeone A, Acampora D, Mallamaci A, Stornaiuolo A, D'Apice MR, Nigro V, & Boncinelli E (1993). A vertebrate gene related to orthodenticle contains a homeodomain of the bicoid class and demarcates anterior neuroectoderm in the gastrulating mouse embryo. The EMBO Journal, 12(7), 2735–2747. 10.1002/j.1460-2075.1993.tb05935.x [PubMed: 8101484]

Simeone A, D'Apice MR, Nigro V, Casanova J, Graziani F, Acampora D, & Avantaggiato V (1994). Orthopedia, a novel homeobox-containing gene expressed in the developing CNS of both mouse and Drosophila. Neuron, 13(1), 83–101. 10.1016/0896-6273(94)90461-8 [PubMed: 7913821]

Siskos N, Ververidis C, Skavdis G, & Grigoriou ME (2021). Genoarchitectonic compartmentalization of the embryonic telencephalon: Insights from the domestic cat. Frontiers in Neuroanatomy, 15, 785541. 10.3389/fnana.2021.785541 [PubMed: 34975420]

Smeets WJ, Marín O, & González A (2000). Evolution of the basal ganglia: New perspectives through a comparative approach. Journal of Anatomy, 196 (Pt 4)(Pt 4), 501–517. 10.1046/j.1469-7580.2000.19640501.x

Smith OC (1930). The corpus striatum, amygdala, and stria terminalis of Tamandua tetradactyla. Journal of Comparative Neurology 51 (1), 65–127. 10.1002/cne.900510104

Spatz H (1921). Zur Anatomie der Zentren des Streifenhügels. Münchener Medizinisches Wochenschrift 45, 1441–1446.

Spatz H (1922). Über Beziehungen zwischen der Substantia nigra des Mittelhirnfusses und dem Globus pallidus des Linsenkerns. Ergänzungs-Heft des Anatomischer Anzeiger: vol 55.

Spatz H (1924). Zur Ontogenese des Striatums und des Pallidums. Deutsche Zeitschrift für Nervenheilkunde, 81, 185–188

Spatz H (1925). Entwicklungsgeschichte der Basalen Ganglien des Menschlichen Grosshirns. Anatomischer Anzeiger Supplement, 60, 54.

Stephenson-Jones M, Samuelsson E, Ericsson J, Robertson B, & Grillner S (2011). Evolutionary conservation of the basal ganglia as a common vertebrate mechanism for action selection. Current Biology: CB, 21(13), 1081–1091. 10.1016/j.cub.2011.05.001 [PubMed: 21700460]

Striedter GF & Northcutt RG (2020). Brains Through Time: A Natural History of Vertebrates. Oxford University Press. 10.1093/oso/9780195125689.001.0001

Stühmer T, Anderson SA, Ekker M, & Rubenstein JLR (2002). Ectopic expression of the Dlx genes induces glutamic acid decarboxylase and Dlx expression. Development, 129(1), 245–252. 10.1242/dev.129.1.245 [PubMed: 11782417]

Stühmer T, Puelles L, Ekker M, & Rubenstein JLR (2002). Expression from a Dlx gene enhancer marks adult mouse cortical GABAergic neurons. Cerebral Cortex, 12(1), 75–85. 10.1093/cercor/12.1.75 [PubMed: 11734534]

Su-Feher L, Rubin AN, Silberberg SN, Catta-Preta R, Lim KJ, Ypsilanti AR, Zdilar I, McGinnis CS, McKinsey GL, Rubino TE, Hawrylycz MJ, Thompson C, Gartner ZJ, Puelles L, Zeng H, Rubenstein JLR, & Nord AS (2022). Single cell enhancer activity distinguishes GABAergic and cholinergic lineages in embryonic mouse basal ganglia. Proceedings of the National Academy of Sciences of the United States of America, 119(15), e2108760119. 10.1073/pnas.2108760119 [PubMed: 35377797]

Sugahara F, Murakami Y, Pascual-Anaya J, & Kuratani S (2022). Forebrain architecture and development in cyclostomes, with reference to the early morphology and evolution of the vertebrate head. Brain, Behavior and Evolution, 96(4–6), 305–317. 10.1159/000519026 [PubMed: 34537767]

Suryanarayana SM, Pérez-Fernández J, Robertson B, & Grillner S (2022). The lamprey forebrain—evolutionary implications. Brain, Behavior and Evolution, 96(4–6), 318–333. 10.1159/000517492 [PubMed: 34192700]

Sussel L, Marin O, Kimura S, & Rubenstein JL (1999). Loss of Nkx2.1 homeobox gene function results in a ventral to dorsal molecular respecification within the basal telencephalon: Evidence

for a transformation of the pallidum into the striatum. Development 126(15), 3359–3370. 10.1242/dev.126.15.3359 [PubMed: 10393115]

Swanson LW (2003). Brain Architecture: Understanding the Basic Plan. Oxford University Press.

Takamori S, Rhee JS, Rosenmund C, & Jahn R (2000). Identification of a vesicular glutamate transporter that defines a glutamatergic phenotype in neurons. Nature, 407(6801), 189–194. 10.1038/35025070 [PubMed: 11001057]

Talbot K & Butcher LL (1978). Nucleus of the crus cerebri: A previously undiscovered cell group forming a reticulum around motor system fibers derived from the cerebral cortex and neostriatum. Neuroscience Abstracts, 4, 306.

Timsit SG, Bally-Cuif L, Colman DR, & Zalc B (1992). DM-20 mRNA is expressed during the embryonic development of the nervous system of the mouse. Journal of Neurochemistry, 58(3), 1172–1175. 10.1111/j.1471-4159.1992.tb09378.x [PubMed: 1737990]

Timsit S, Martinez S, Allinquant B, Peyron F, Puelles L, & Zalc B (1995). Oligodendrocytes originate in a restricted zone of the embryonic ventral neural tube defined by DM-20 mRNA expression. Journal of Neuroscience, 15(2), 1012–1024. 10.1523/JNEUROSCI.15-02-01012.1995 [PubMed: 7869079]

Turner KJ, Hawkins TA, Yáñez J, Anadón R, Wilson SW, & Folgueira M (2016). Afferent connectivity of the zebrafish habenulae. Frontiers in Neural Circuits, 10, 30. 10.3389/fncir.2016.00030 [PubMed: 27199671]

van den Akker WMR, Brox A, Puelles L, Durston AJ, & Medina L (2008). Comparative functional analysis provides evidence for a crucial role for the homeobox gene Nkx2.1/Titf-1 in forebrain evolution. Journal of Comparative Neurology, 506(2), 211–223. 10.1002/cne.21542 [PubMed: 18022953]

van der Kooy D, & Carter DA (1981). The organization of the efferent projections and striatal afferents of the entopeduncular nucleus and adjacent areas in the rat. Brain Research, 211(1), 15–36. 10.1016/0006-8993(81)90064-0 [PubMed: 6164450]

Villar-Cerviño V, Holstein GR, Martinelli GP, Anadón R, & Rodicio MC (2008). Glycine-immunoreactive neurons in the developing spinal cord of the sea lamprey: Comparison with the gamma-aminobutyric acidergic system. Journal of Comparative Neurology, 508(1), 112–130. 10.1002/cne.21661 [PubMed: 18302155]

Vincent SR, & Brown JC (1986). Somatostatin immunoreactivity in the entopeduncular projection to the lateral habenula in the rat. Neuroscience Letters, 68(2), 160–164. 10.1016/0304-3940(86)90134-5 [PubMed: 2875419]

Wallace ML, Saunders A, Huang KW, Philson AC, Goldman M, Macosko EZ, McCarroll SA, & Sabatini BL (2017). Genetically distinct parallel pathways in the entopeduncular nucleus for limbic and sensorimotor output of the basal ganglia. Neuron, 94(1), 138–152.e5. 10.1016/j.neuron.2017.03.017 [PubMed: 28384468]

Wang W, & Lufkin T (2000). The murine Otp homeobox gene plays an essential role in the specification of neuronal cell lineages in the developing hypothalamus. Developmental Biology, 227(2), 432–449. 10.1006/dbio.2000.9902 [PubMed: 11071765]

Watanabe K, & Kawana E (1982). The accessory nucleus of Luys in the rat. Okajimas Folia Anatomica Japonica, 58(4–6), 859–874. 10.2535/ofaj1936.58.4-6_859 [PubMed: 7122020]

Watts AG, & Swanson LW (1987). Efferent projections of the suprachiasmatic nucleus: II. Studies using retrograde transport of fluorescent dyes and simultaneous peptide immunohistochemistry in the rat. Journal of Comparative Neurology, 258(2), 230–252. 10.1002/cne.902580205 [PubMed: 2438309]

Watts AG, Swanson LW, & Sanchez-Watts G (1987). Efferent projections of the suprachiasmatic nucleus: I. Studies using anterograde transport of Phaseolus vulgaris leucoagglutinin in the rat. Journal of Comparative Neurology, 258(2), 204–229. 10.1002/cne.902580204 [PubMed: 3294923]

Wyss JM, & Sripanidkulchai B (1985). An autoradiographic analysis of the time of origin of neurons in the hypothalamus of the cat. Brain Research, 353(1), 89–98. 10.1016/0165-3806(85)90026-4 [PubMed: 4027685]

Xu H, Zheng F, Krischek B, Ding W, Xiong C, Wang X, & Niu C (2017). Subthalamic nucleus and globus pallidus internus stimulation for the treatment of Parkinson's disease: A systematic review. Journal of International Medical Research, 45(5), 1602–1612. 10.1177/0300060517708102 [PubMed: 28701061]

Xu Q, Tam M, & Anderson SA (2008). Fate mapping Nkx2.1-lineage cells in the mouse telencephalon. Journal of Comparative Neurology, 506(1), 16–29. 10.1002/cne.21529 [PubMed: 17990269]

Zaborszky L, van del Pool A, & Gyengesi E (2012). The basal forebrain cholinergic projection system in mice. In Watson C, Paxinos G, & Puelles L (Eds.), The Mouse Nervous System (pp. 684–718). Elsevier Academic Press. 10.1016/B978-0-12-369497-3.10028-7

Zerucha T, Stühmer T, Hatch G, Park BK, Long Q, Yu G, Gambarotta A, Schultz JR, Rubenstein JL, & Ekker M (2000). A highly conserved enhancer in the Dlx5/Dlx6 intergenic region is the site of cross-regulatory interactions between Dlx genes in the embryonic forebrain. Journal of Neuroscience, 20(2), 709–721. [PubMed: 10632600]

Zhang J, Li J, Chen F, Liu X, Jiang C, Hu X, Ma L, & Xu Z (2021). STN versus GPi deep brain stimulation for dyskinesia improvement in advanced Parkinson's disease: A meta-analysis of randomized controlled trials. Clinical Neurology and Neurosurgery, 201, 106450. 10.1016/j.clineuro.2020.106450 [PubMed: 33421741]

Zhao T, Szabó N, Ma J, Luo L, Zhou X, & Alvarez-Bolado G (2008). Genetic mapping of Foxb1-cell lineage shows migration from caudal diencephalon to telencephalon and lateral hypothalamus. European Journal of Neuroscience, 28(10), 1941–1955. 10.1111/j.1460-9568.2008.06503.x [PubMed: 19046377]

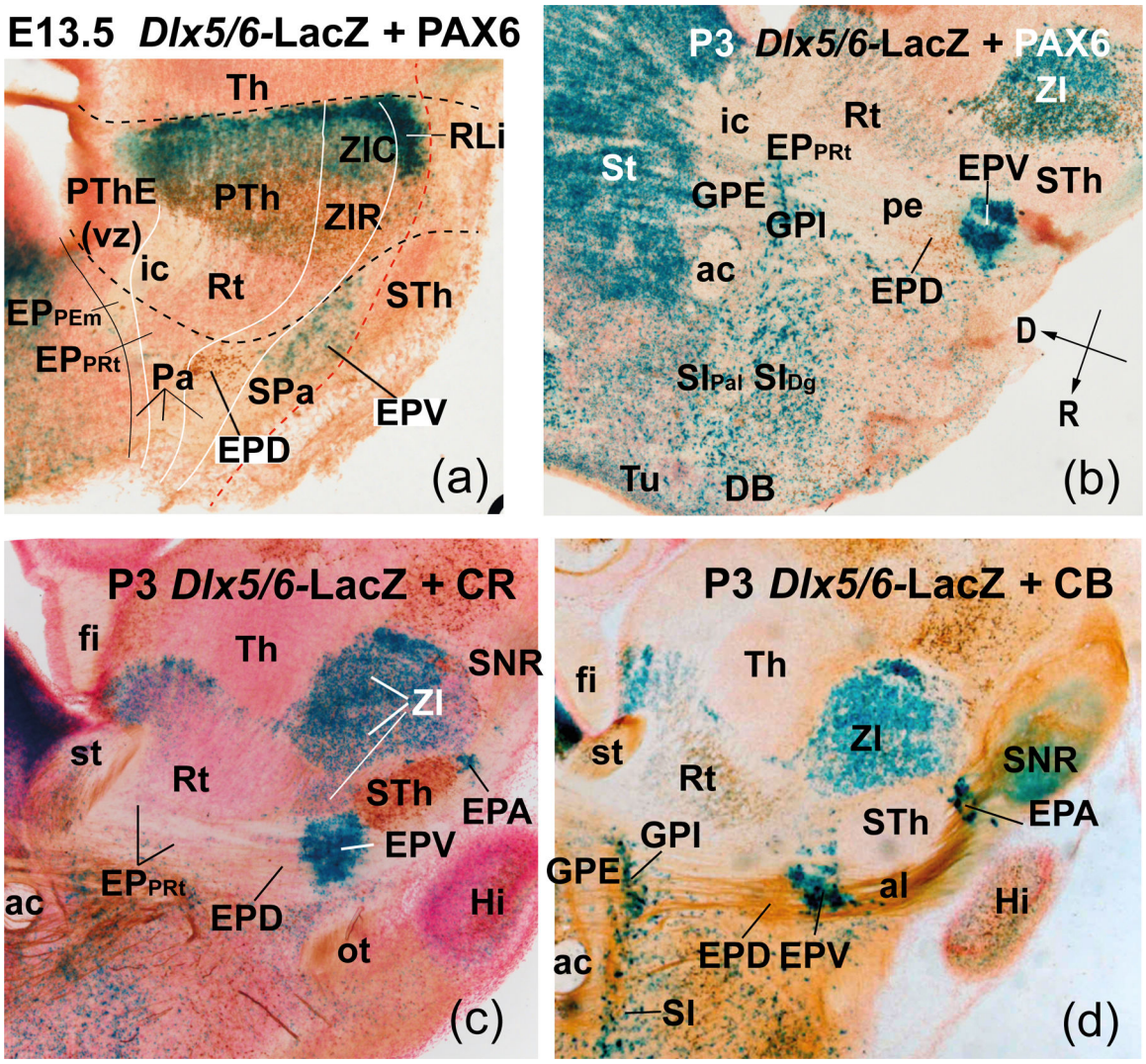

FIGURE 1.

Panels illustrating entopeduncular cell subpopulations of the alar hypothalamus in embryonic and postnatal mouse stages carrying a *Dlx5/6*-LacZ construct combined with immunohistochemistry for specified markers. The sections were counterstained with neutral red. Dorsal and rostral directions are indicated in (**b**). (**a**) A sagittal section of an embryonic brain at E13.5 showing *Dlx5/6*-LacZ-expressing cells (blue) in the ventral entopeduncular nucleus (EPV) and PAX6-positive cells (brown) in the dorsal entopeduncular nucleus (EPD); note the pre-reticular (EP_{PRt}) and pre-eminential (EP_{PEm}) nuclei are both unlabeled. (**b**) LacZ signal and PAX6-immunostainning in EPV and EPD cells respectively in a sagittal section of a postnatal day 3 (P3) brain. Note the globus pallidus is a distinct telencephalic entity subdivided into an internal triangular large-celled part (GPI) and an external quadrangular part (GPE) with medium-sized cells. Both parts contain LacZ-positive cells. GPI belongs to the diagonal radial histogenetic domain which also contains a part of the BST complex (not shown), the posterior substantia innominata part (SI_{Dg}) and the subpial diagonal band (DB); GPE forms part of the pallidal radial histogenetic domain containing also part of the BST complex (not shown), the rostral substantia innominata (SI_{PAL}) and a

small rostral part of the diagonal band formation (DB) apart of ectopic derivatives within the deep stratum of the olfactory tuberculum. (**c, d**) *Dlx5/6*-LacZ reaction combined with calretinin (CR) immunostaining in (**c**) and with calbindin (CB) immunostaining in (**d**) in two consecutive sagittal sections at P3. Blue LacZ signal is restricted to EPV and a neighboring basal prethalamic population lying caudal to the subthalamic nucleus (STh), identified as the accessory entopeduncular nucleus (EPA). EPD cells are CB-positive and CR-negative. Note large LacZ-positive GPI cells in (**d**). See the list of abbreviations for other tags.

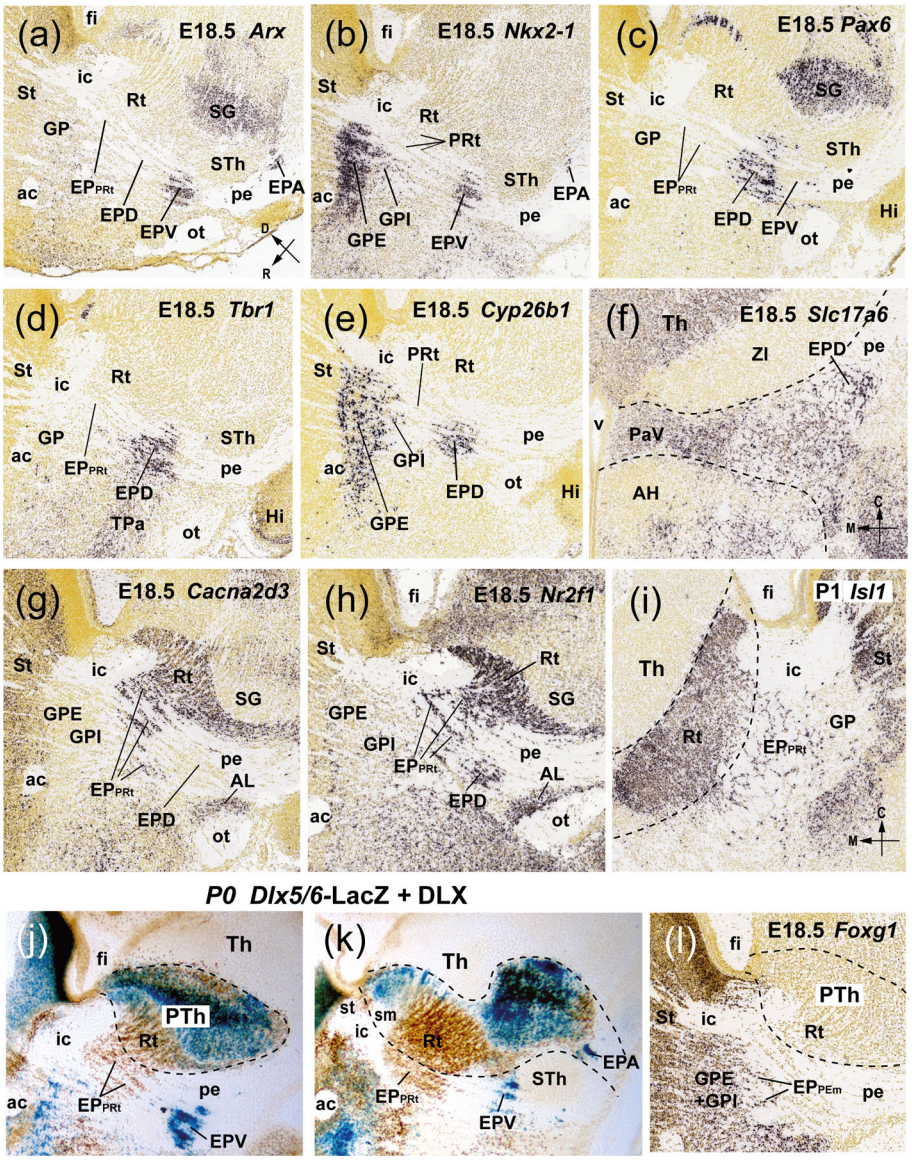

FIGURE 2.

Differential molecular characterization of the four entopeduncular cell populations (ventral -EPV, dorsal -EPD, pre-reticular -EP_{PRt}, pre-eminential -EP_{PEm}) in the alar hypothalamus of the mouse. These sections were downloaded from the Allen Developing Mouse Brain Atlas (http://developingmouse.brain-map.org/experiment/show/ experiment number). Dorsal and rostral directions in the sagittal sections are indicated in (**a**); caudal and medial directions in horizontal sections through the hypothalamus are indicated in (**f**) and (**i**). (**a, b**) *Arx*- and *Nkx2-1*-expressing cells in EPV in sagittal sections at E18.5 (experiments 100056265 and 100056265, respectively). (**c, d, e**) *Pax6*-, *Tbr1*-, and *Cyp26b1*-positive cells in EPD in three sagittal sections also at E18.5 (experiments 100085451, 100029446, and 100054745, respectively). (**f**) Expression of the glutamatergic *Slc17a6* cotransporter in the hypothalamic paraventricular (Pa) domain in a horizontal section through the ventral subdivision of this formation (PaV) at E18.5 (experiment 100059213). Note *Slc17a6*-expressing cells in EPD

within the superficial part of the radial Pa domain. (**g, h**) *Cacna2d3*- and *Nr2f1*-positive cells in the EP_{PRt} located dorsal to EPD and rostral to the prethalamic reticular nucleus (Rt) whose cells are also positive (experiments 100090618 and 100071564, respectively. Note EPD cells lack *Cacna2d3*-expression but are *Nr2f1*-positive. (**i**) Horizontal section through the central (middle) dorsoventral part of the hypothalamic paraventricular area (PaC) containing EP_{PRt} *Isl1*-expressing cells next to prethalamic Rt *Isl1*-positive cells at P1 (experiment 100091995). (**j**, **k**) Two sagittal sections through the hypothalamus of a P0 mouse brain showing *Dlx5/6*-LacZ-related β-galactosidase activity (blue) and reacted with an anti-Distalless (DLX) polyclonal antibody that recognizes all forms of DLX (brown; modified from Puelles et al. 2021; their Figure 5b,c). (**j**) is lateral to (**k**). Note EP_{PRt} cell are only DLX-immunopositive (possible selective presence of Dlx1) whereas EPV and EPA cells contain strong LacZ signal (Dlx5/6). (**l**) A sagittal section of a E18.5 mouse brain illustrating *Foxg1*-expressing cells in the EP_{PEm} subjacent to the globus pallidus (GPE+GPI) (experiment 100072314). For additional abbreviations see list.

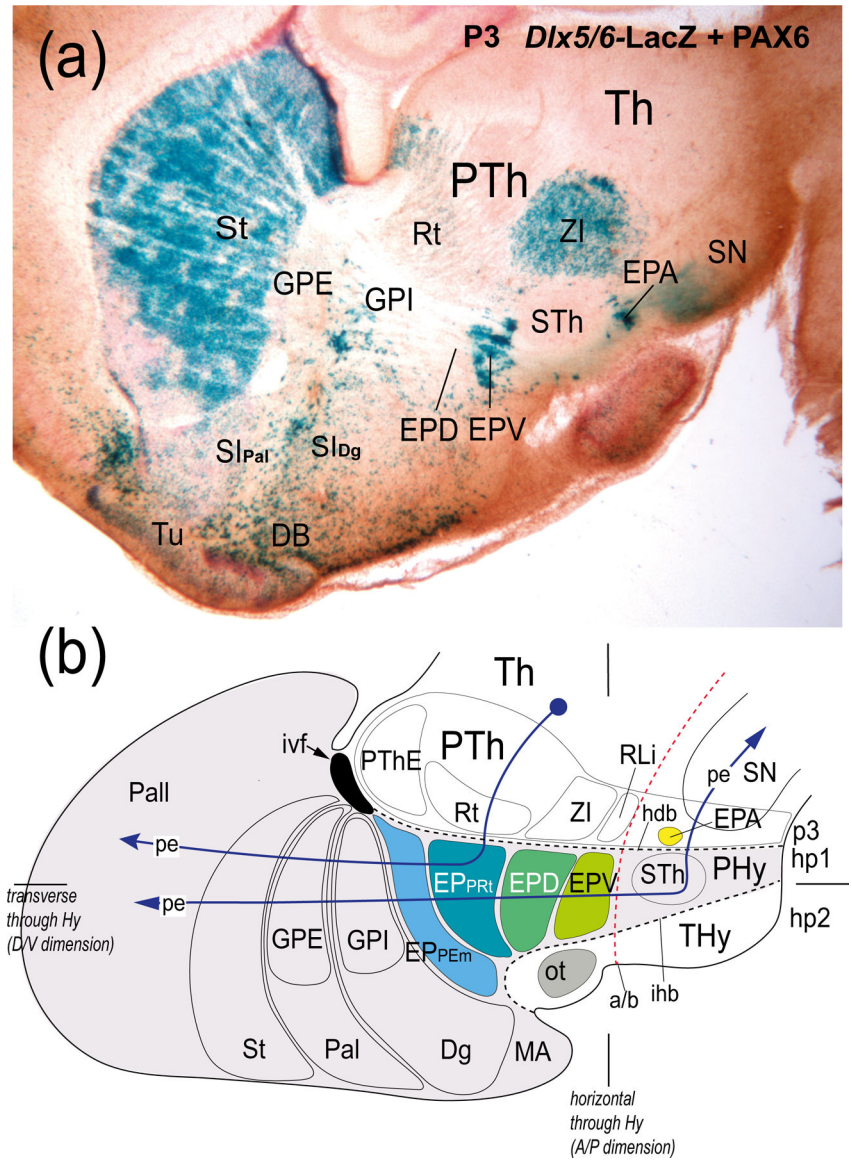

FIGURE 3.

Photograph and schema summarizing the double nature of the globus pallidus and quadruple dorsoventral subdivision of the alar entopeduncular hypothalamic subpopulations, plus the prethalamic accessory entopeduncular component (EPA). (**a**) A sagittal section of Dlx5/6-LacZ material at P3 shows distinctly the striatal, pallidal and diagonal subpallial domains extending from the ventricle to the pial surface, jointly with the intrahypothalamic peduncle and related grisea. The photo displays the two parts of the globus pallidus (external and internal -GPE, GPI, with the larger neurons of GPI being more reactive for beta-galactosidase than the GPE population) as well as the equally Dlx5/6-LacZ-positive EPV and EPA formations. The large space along the peduncle between GPI and EPV is occupied by the EP_{PEm}, the EP_{PRt}, and the EPD, in dorsoventral order. The structure separating EPV from EPA is the subthalamic nucleus (STh). The rostral pole of the substantia nigra is seen just behind EPA (with bluish neuropile stain due to anterograde transport of

beta-galactosidase reaction product). Note also the neighboring position of the prethalamic reticular nucleus (where Dlx5/6-LacZ signal was largely downregulated) and zona incerta (still LacZ-positive). (**b**) The schema summarizes all these entities (pre-eminential, EP_{PEm}; pre-reticular. EP_{PRt}; dorsal entopeduncular, EPD; ventral entopeduncular, EPV), correlating each alar entopeduncular subdivision with a specific caudal alar prethalamic entity; in dorsoventral order we see the prethalamic eminence (PThE), the reticular nucleus (Rt), the incertal complex (ZI) and the rostral liminar band (RLi). Dark blue lines indicate the trajectory of the lateral forebrain bundle (peduncle, pe) wherein entopeduncular hypothalamic cells are immersed. An accessory entopeduncular nucleus (EPA) lies nearby within the prethalamic tegmentum (i.e., in prosomere 3, p3). The internal component of the globus pallidus (GPI) lies immediately dorsal to the EP_{PEm} hypothalamic subdivision. Note the longitudinal dimension is given by the red dashed line representing the alar-basal boundary. Transverse and horizontal topological planes in the schema B (according to the prosomeric model), indicate also that the transverse plane represents the DV dimension and the horizontal plane the AP dimension. For additional abbreviations see list.

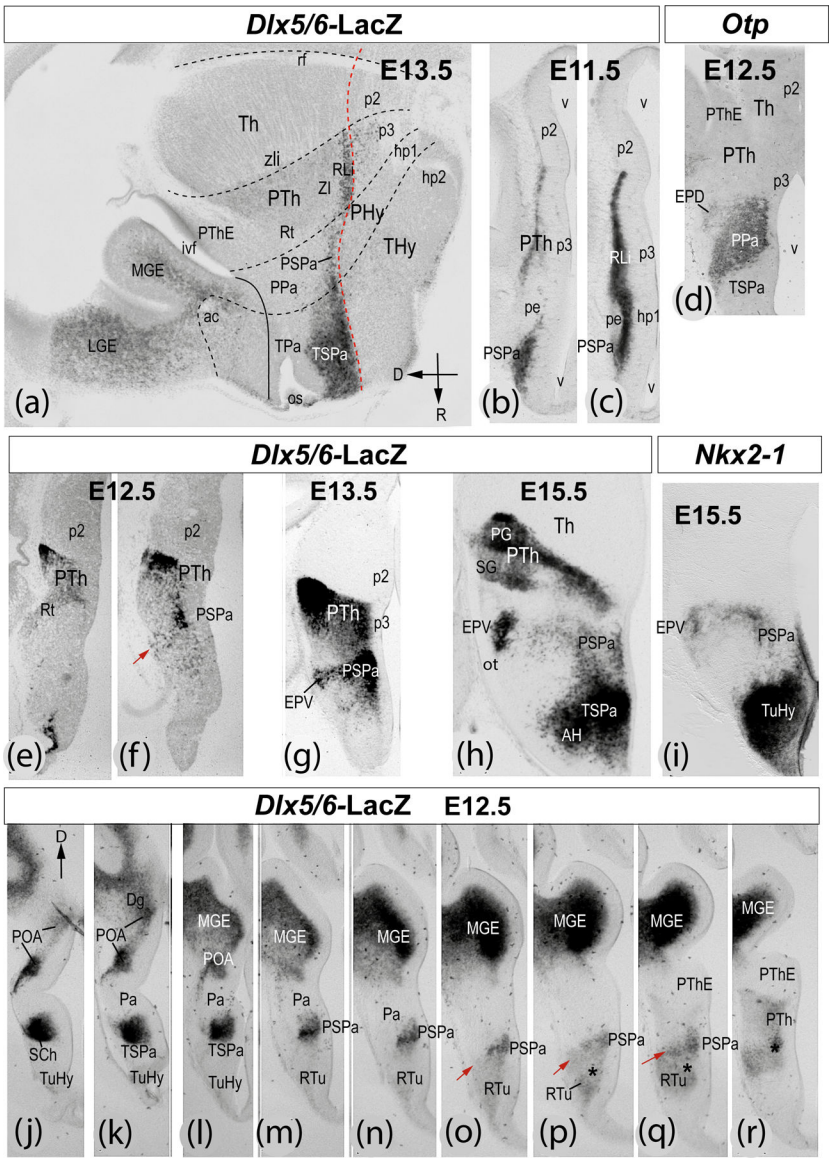

FIGURE 4.

Panels illustrating the embryonic development of the ventral entopeduncular nucleus (EPV) using mouse embryos carrying a *Dlx5/6*-LacZ transgenic construct reacted to show β-galactosidase activity. (**a**) A sagittal overview of the *Dlx5/6*-LacZ signal in the hypothalamic subparaventricular domain (SPa) at E13.5. Note the terminal part of SPa (TSPa; later subdivided into the suprachiasmatic and anterior nuclei) is wider compared to the narrow peduncular part of SPa (PSPa). The PSPa contacts caudally the similarly LacZ reactive prethalamic rostral liminar band (RLi). The red dashed line indicates the alar/basal limit. Black dashed lines indicate the interneuromeric thalamo-pretectal, interthalamic, prethalamo-hypothalamic, and intrahypothalamic limits according to the prosomeric model. Dorsal (D) and rostral (R) directions are indicated. (**b**, **c**) Two horizontal sections through the peduncular hypothalamus (hypothalamo-telencephalic prosomere 1 or hp1), and the diencephalic prosomeres 2 and 3 (p2, p3) showing the longitudinal LacZ signal restricted

to SPa and the prethalamic RLi at E11.5; note also the slight superficial indentation of the LacZ-positive mantle band at the peduncular locus of the incipient cerebral peduncle (pe). (**d**) Expression of *Otp* mRNA in a horizontal section through the peduncular hypothalamic paraventricular domain (PPa) at E12.5; *Otp*-expressing cells appear in the dorsal entopeduncular nucleus (EPD), superficial to the main PPa. (**e**, **f**) *Dlx5/6*-LacZ signal in the PTh and PSPa at E12.5. A red arrow indicates the location of the early ventral entopeduncular nucleus primordium (EPV). (**g, h**) Horizontal sections through the PSPA and PTh showing increase of LacZ signal in the EPV at E13.5 and E15.5, respectively. (**i**) Oblique section through the alar PSPA and the basal tuberal hypothalamic region (Tu) showing *Nkx2-1* in a subpopulation of EPV cells at E15.5. (**j**-**r**) Slightly oblique series of transversal sections (parallel to the peduncular course) from a E12.5 mouse brain reacted for *Dlx5/6*-LacZ signal. Dorsal (D) direction is indicated. The red arrows indicate the superficial EPV primordium emerging within the PSPa; the asterisk indicates the periventricular retrotuberal (RTu) zone. See the list for additional abbreviations.

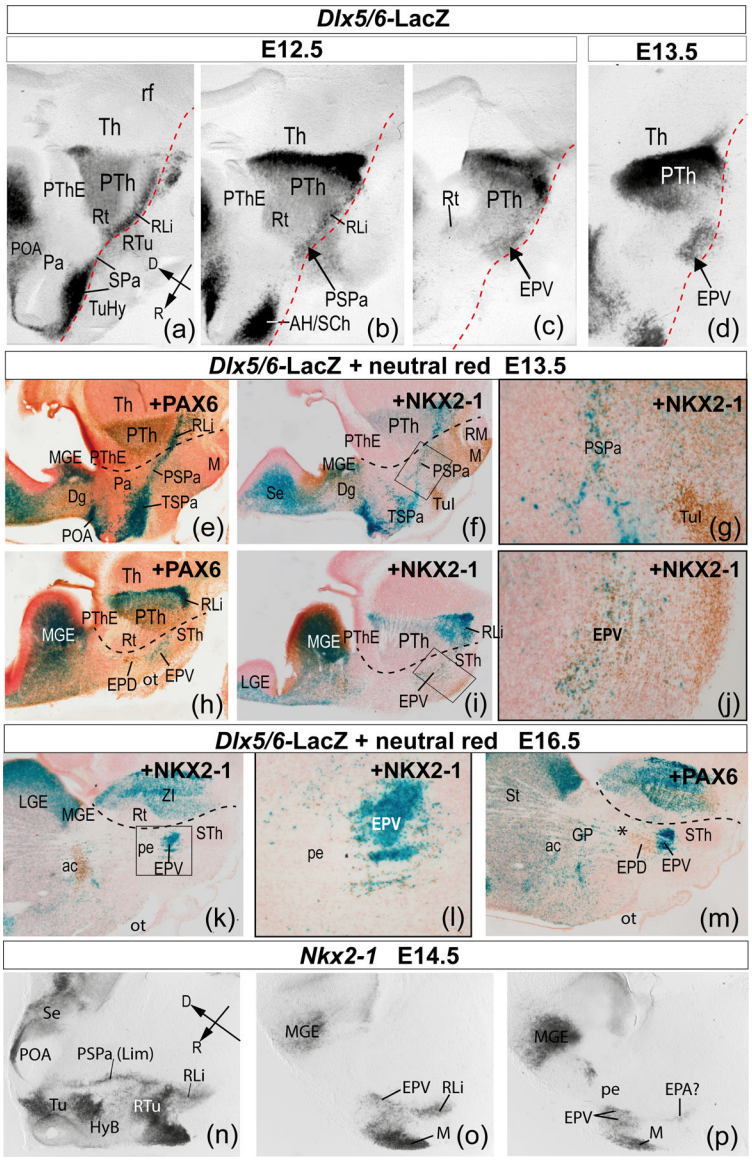

FIGURE 5.

Molecular characterization of the ventral entopeduncular nucleus (EPV) at various embryonic stages. (**a**-**d**) Sagittal sections of *Dlx5/6*-LacZ transgenic mice at E12.5 and E13.5 showing the superficial EPV primordium associated to the peduncular subparaventricular domain (PSPa). The rostral (R) and dorsal (D) directions are indicated in (**a**) (**e**-**j**) Medial (**e**, **f**) and lateral (**h**, **i**) sagittal sections from two *Dlx5/6*-LacZ mice further immunoreacted for PAX6 or NKX2-1 antibodies. EPV cells contain LacZ and NKX2-1 signals whereas the dorsal entopeduncular nucleus (EPD) only contains PAX6-positive neurons. (**g**, **j**) Higher magnification of the boxes indicated in (**f**) and (**i**), respectively. (**k**) Sagittal section of a *Dlx5/6*-LacZ mouse immunoreacted for NKX2-1. (**l**) Higher magnification of the box indicated in (**k**) showing LacZ and NKX2-1 signals in EPV cells. (**m**) Differential LacZ and PAX6 signals in the EPV and EPD, respectively. (**n**-**p**) In situ hybridization for *Nkx2-1* in sagittal sections of a E14.5 mouse brain showing

Nkx2-1-positive cells in the EPV which are superficial to the liminar PSPa band (Lim = the ventralmost part of the PSPa). The rostral (R) and dorsal (D) directions are indicated in (**n**) See the list for additional abbreviations.

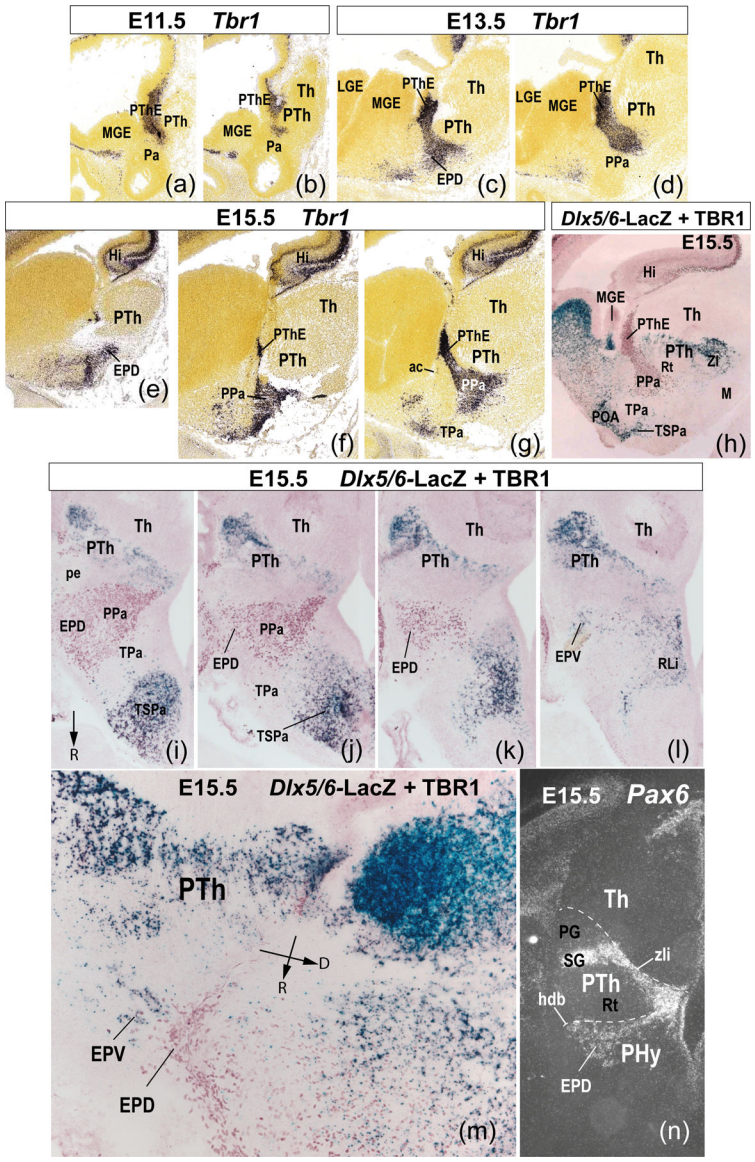

FIGURE 6.

Molecular characterization of the dorsal entopeduncular nucleus (EPD) at various embryonic stages in the mouse brain. (**a**, **b**) *Tbr1* expression in two lateromedial sagittal sections of a E11.5 mouse brain (experiment 100092710). *Tbr1* expression is mainly restricted to the prethalamic eminence (PThE) with potential tangentially migrated cells in the paraventricular hypothalamic domain (Pa). (**c**, **d**) *Tbr1* expression at E13.5 in the PThE and the superficial EPD locus within the peduncular Pa domain (experiment 100024822). (**e-g**) *Tbr1*-expressing cells in the EPD within the peduncular Pa domain (PPa) at E15.5. Sections shown in (**a-g**) were downloaded from the Allen Developing Mouse Brain Atlas (http://developingmouse.brain-map.org/experiment/show/ experiment number). (**h**) TBR1-immunoreaction (in red) in a sagittal section of a *Dlx5/6*-LacZ mouse (blue reaction) at E15.5; note differential dorsoventral positions. (**i-l**) Four dorsoventrally ordered horizontal sections through the hypothalamus of a E15.5 *Dlx5/6*-LacZ mouse further immunoreacted

for TBR1 antibody. TBR1-immunoreacted cells (red) of the EPD and LacZ signal (blue) in the EPV are illustrated. The rostral (R) direction is indicated in (**i**) (**m**) Higher magnification of an oblique section through the hypothalamus showing *Dlx5/6*-LacZ and TBR1 reactions in EPV and EPD, respectively. The rostral (R) and dorsal (D) directions are indicated. (**n**) *Pax6* in situ hybridization in a horizontal section through the peduncular hypothalamus (PHy) at E15.5, illustrating *Pax6*-expressing cells in the EPD. Note the neighboring prethalamus (PTh) lacks *Pax6* expression excepting the subgeniculate nucleus (SG). See the list for additional abbreviations.

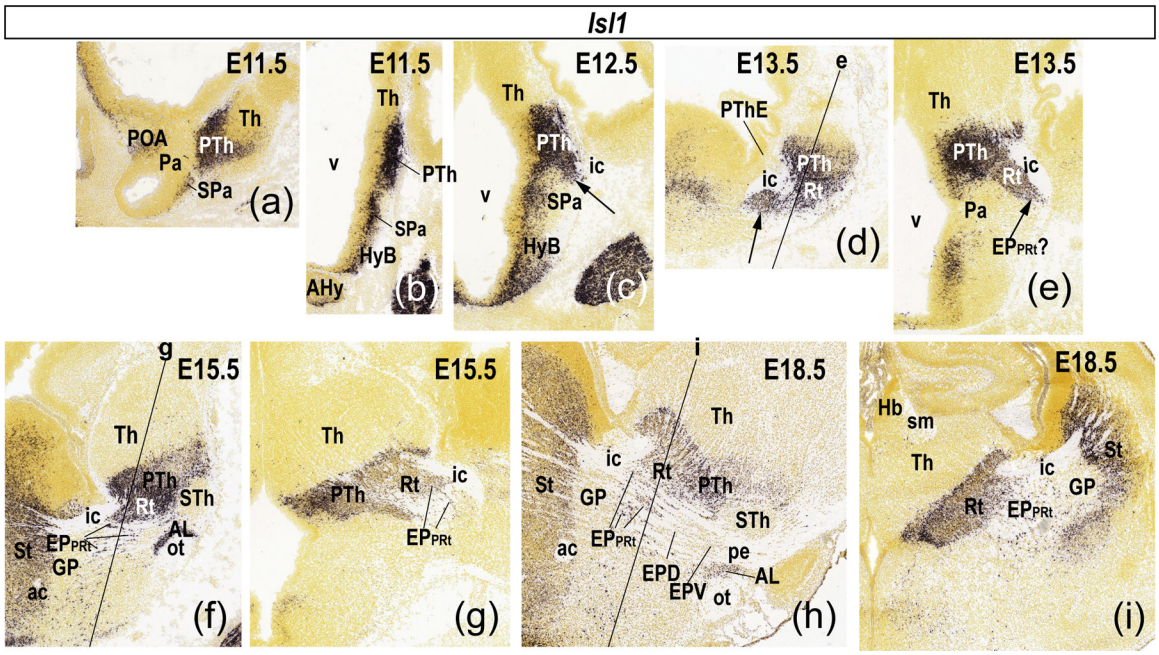

FIGURE 7.

Expression of *Isl1* in the pre-reticular entopeduncular nucleus (EP_{PRt}) at embryonic stages. All images were downloaded from the Allen Developing Mouse Brain Atlas (http://developingmouse.brain-map.org/experiment/show/experiment number). (**a**) A lateral sagittal section through the *Isl1*-expressing prethalamus (PTh) and the hypothalamic subparaventricular domain (SPa) at E11.5 (experiment 100029096). (**b, c**) Horizontal sections at E11.5 (experiment 100091545) and E12.5 (experiment 100091110) showing strong *Isl1* expression in PTh, SPa and the basal hypothalamus (HyB). Black arrow in (**c**) indicates potential cells migrated from the PTh in the superficial SPa. (**d, e**) Sagittal and horizontal sections (experiments 100093279 and 100091551, respectively) showing *Isl1*-expressing cells in the prethalamic reticular nucleus (Rt) and positive possible migrated cells in the EP_{PRt} (black arrows). (**f**, **g**) Sagittal and horizontal sections showing dispersed *Isl1*-positive cells intermingled among the unlabeled fibers of the cerebral peduncle (pe) in a prereticular position (EP_{PRt} nucleus); (f, g) correspond respectively to experiments 100085330 and 100092145). (**h**, **i**) Sagittal and horizontal sections showing dispersed *Isl1*-positive EP_{PRt} cells intermingled with peduncular fibers, rostral to *Isl1*-expressing Rt cells and ventral to the unlabeled globus pallidus complex (GP), (h, i) correspond respectively to experiments 100032051 and 100092412). See the list for additional abbreviations.

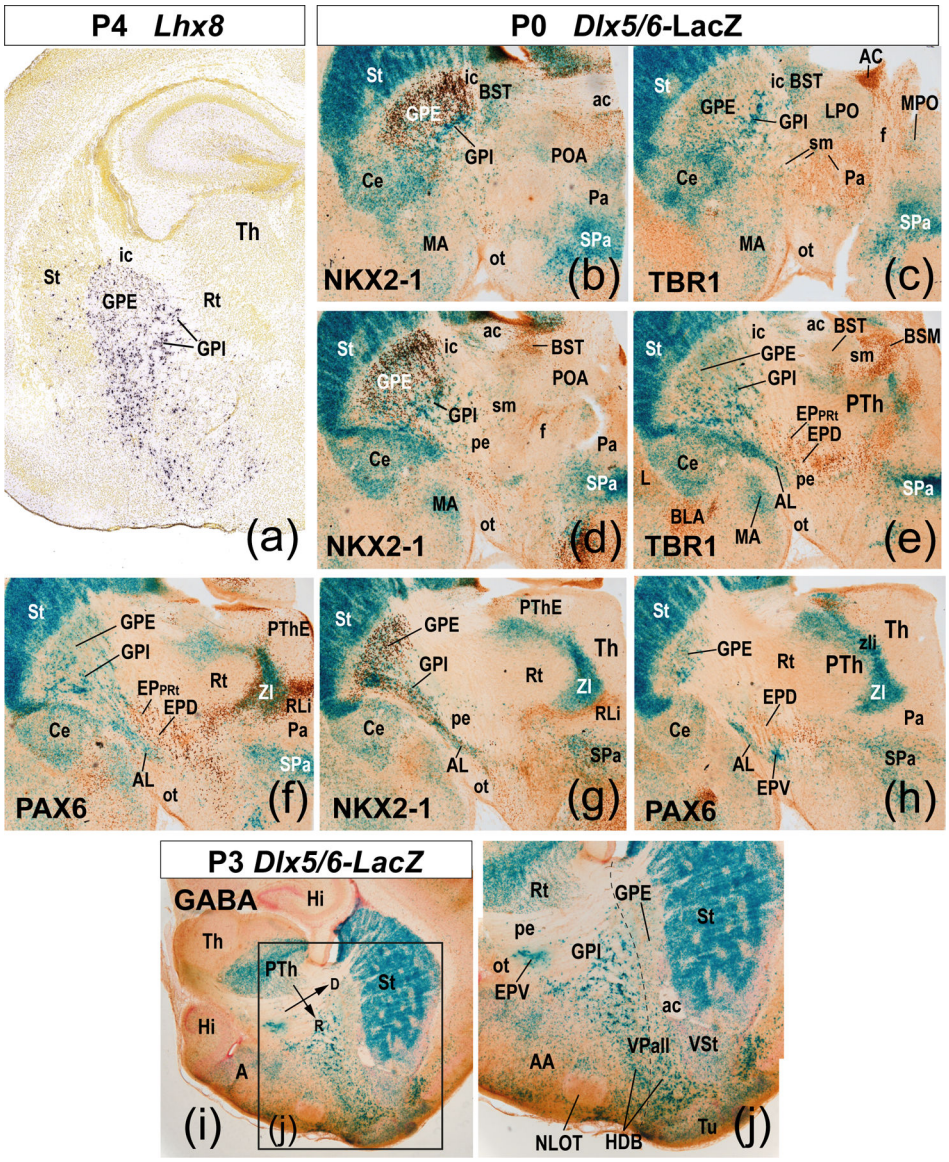

FIGURE 8.

Differential molecular characterization of the mouse external and internal globus pallidus (GPE, GPI) and dorsal and ventral entopeduncular nuclei (EPD, EPV) at diverse postnatal stages. (**a**) *Lhx8* expressing cells in the GPE and GPI in a coronal section through the subpallium and alar diencephalon at P4. Note GPI-positive cells are larger than GPE-positive cells. Section (a) was downloaded from the Allen Mouse Brain Atlas. (**b**-**g**) Oblique sections illustrating the telencephalic striatum (St), the GPE/GPI pair, and the preoptic area (POA) in relation to the hypothalamic paraventricular and subparaventricular domains (Pa; containing EPD cells; SPa; containing EPV cells) in a P0 *Dlx5/6*-LacZ transgenic mouse. The sections where immunoreacted for NKX2-1 (**b**, **d**, **g**), TBR1 (**c**, **e**) and PAX6 (**f**, **h**). The GP complex contains both LacZ and NKX2-1 signals and is subdivided into GPI (with large cells) and GPE (with medium-sized cells). EPD contains TBR1- and PAX6-immunoreactive cells. EPV cells are *Dlx5/6*-LacZ-positive. (**i**) Immunoreaction for GABA antibody in a sagittal

section, counterstained with neutral red in a P3 *Dlx5/6*-LacZ mouse. The rostral (R) and dorsal (D) directions are indicated. The box is magnified in (**j**). GPI is part of the diagonal radial histogenetic domain which contains superficially the larger part of the diagonal band formation (HDB at this level). GPE reaches superficially and radially to the rostral minor part of the diagonal band nucleus. The dash line indicates the approximate diagonal/pallidal limit. See the list for additional abbreviations.

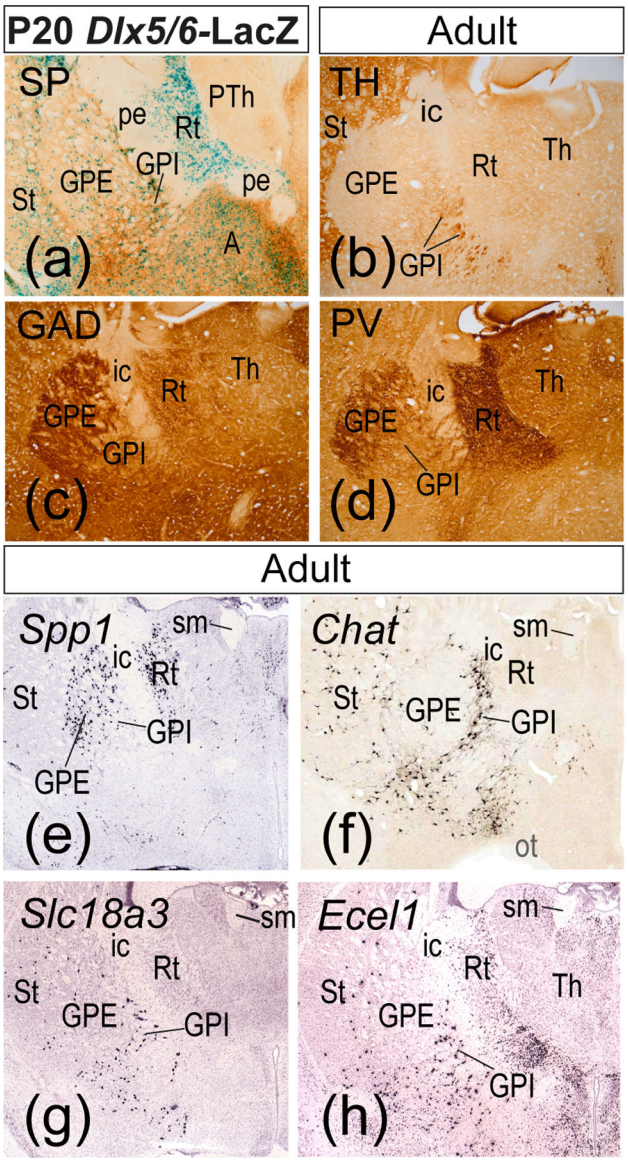

FIGURE 9.

Characterization of the external and internal parts of the globus pallidus (GPE, GPI) in postnatal mouse brains. (**a**) A sagittal section through the subpallial region of a P20 *Dlx5/6*-LacZ mouse further immunoreacted for substance P. LacZ signal labels GABAergic neurons. (**b-d**) Immunohistochemical labeling of tyrosine hydroxylase (TH), glutamic acid decarboxylase (GAD) and parvalbumin (PV) neurons in coronal sections of adult mouse brains. (**e**) Selective expression of *Spp1* in GPE in a coronal section at P56. (**f**) Cholinergic *Chat*-positive GPI neurons in a coronal section of an adult brain. (**g, h**) *Slc18a3* and *Ecel1* expression, respectively, in GPI at P56 in coronal sections at a section level comparable to (**f**); *Slc18a3* encodes a vesicular monoamine transporter. Sections (**e**), (**g**) and (**h**) were downloaded from the Allen Developing Mouse Brain Atlas (http://developingmouse.brain-map.org/gene/show/ experiment number: (e)75651180, (g) 73521822 and (h) 70231305)

whereas section (**f**) is from the GENSAT Project (the Rockefeller University). See the list for additional abbreviations.

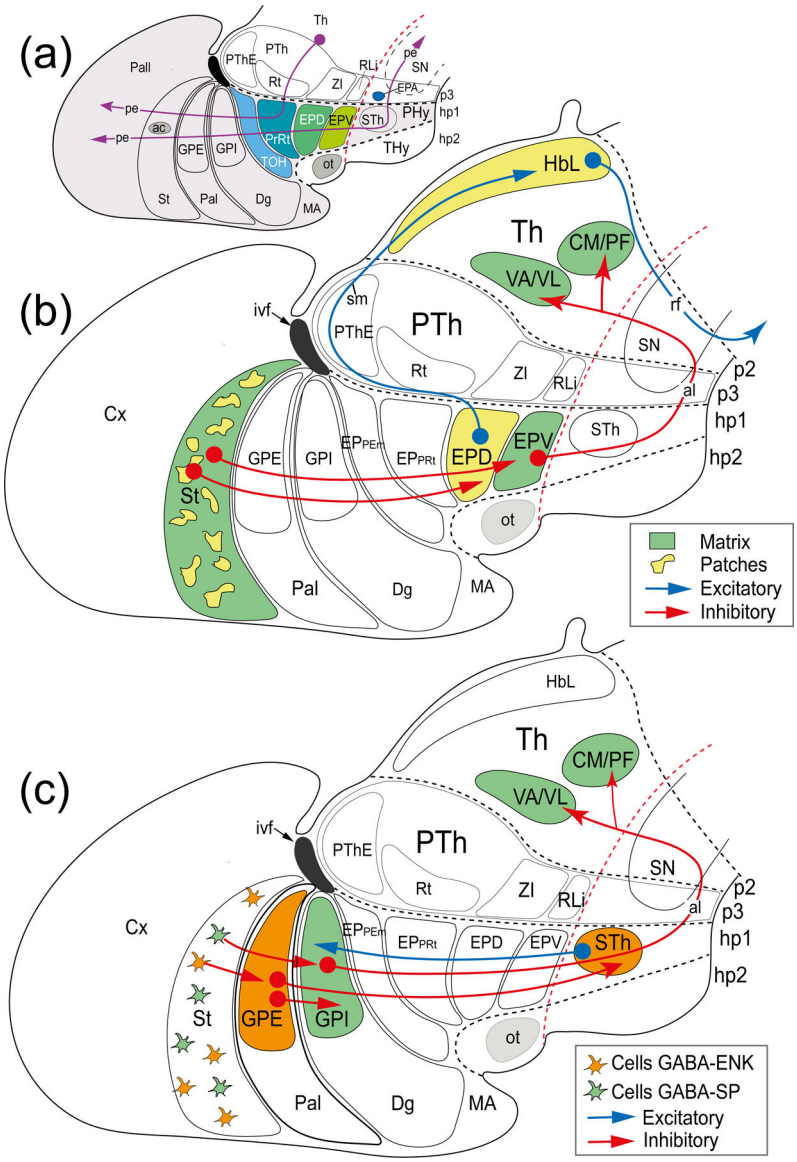

FIGURE 10.

Schemata summarizing similarities and differences in the connectivity of the hypothalamic dorsal and ventral entopeduncular nuclei (EPD, EPV) and the subpallial external and internal globus pallidus parts (GPE, GPI). (**a**) Color-coded schema showing the four alar dorsoventral hypothalamic subpopulations associated to the cerebral peduncle (pe). Each subdivision relates topographically caudally to a prethalamic population: the pre-eminential EP nucleus (EP_{PEm}) to the prethalamic eminence (PThE), the pre-reticular EP nucleus (EP_{PRt}) to the reticular nucleus (Rt), the dorsal EP nucleus (EPD) to the incertal complex (ZI) and the ventral EP nucleus (EPV) to the rostral liminar band (RLi). (**b**) Outputs and inputs of EPD and EPV. The striatal inhibitory inputs originate from either the striatal matrix or striosomal patches. Excitatory EPD outputs target the lateral habenula area (HbL) and inhibitory EPV cells project to some motor thalamic nuclei by the ansa lenticularis (al). (**c**) Outputs and inputs of the GPE and GPI. GPE receives projections from GABAergic

enkephalin (ENK)-containing striatal neurons and GPI cells are targeted by GABAergic substance P (SP)-positive striatal cells. Inhibitory GPE cells project to the hypothalamic subthalamic nucleus (STh) and inhibitory GPI cells project to the thalamus by the ansa lenticularis (al); GPI receives an excitatory input from STh. See the text for References. See the list for additional abbreviations.

TABLE 1.

Antibody list

Antibody	Antigen	Manufacturer, host species, RRID, catalog number, characterization	Diluti
Calbindin (CB)	Recombinant rat calbindin D- 28k.	Swant, Bellinzona, Switzerland, Cat# CB 38; RRID:AB-10000340; rabbit polyclonal; it recognizes a single band of approximately 27–28 kDa in immunoblots. It cross reacts with calbindin D-28k from many other species, including human, monkey, rat, mouse, chicken, and fish.	1:150
Calretinin (CR)	Recombinant human calretinin containing a 6-his tag at the N-terminal.	Swant, Bellinzona, Switzerland, Cat# CR 7697, RRID: AB_2619710 rabbit polyclonal–calcium dependent reaction, code 7696, lot 25392. This antiserum does not cross-react with calbindin D- 28k or other known calcium binding- proteins, as determined by immunoblots and by its distribution in the brain. The antibody was evaluated for specificity and potency by (a) Biotin- Avidin labeling of cryostate-, vibratome, and paraffin sections of 4% paraformaldehyde fixed brains and (b) immunoenzymatic labeling of immunoblots.	1:200
Gamma-Aminobutyric Acid (GABA)	GABA-BSA	Polyclonal rabbit anti-GAD, A2052; Sigma-Aldrich/Merck; RRID: AB_477653 The antibody is isolated from antiserum by immunospecific methods of purification. Antigen specific affinity isolation removes essentially all rabbit serum proteins, including immunoglobulins which do not specifically bind to GABA.anti-GABA shows positive binding with GABA, and GABA-KLH in a dot blot assay, and negative binding with BSA.	1:300

TABLE 2.

Nucleotide sequences of *in situ* hybridization probes

Plasmid name	Source	Insert size in base pairs	cDNA nucleotides of probe or nucleotides from the 3'_ end
Nkx2-1	J.L.R. Rubenstein	2200	Full coding sequence
Otp	A. Simeone	500	500 from 3´ end
Pax6	J.L.R. Rubenstein	2100	2100 from 3´ end

TABLE 3.

Color-coded entries represent large subpopulations (SP) of positive cells for the indicated markers at the specified EP across the hypothalamic and GP sectors.

EP sectors correlates with alar subdivisions of the peduncular hypothalamus (PHy). GP is subdivided in internal and external parts (GPI, GPE). EPA, accessory entopeduncular nucleus; EPD, dorsal entopeduncular nucleus; EP_{PEm}, entopeduncular preeminential nucleus; EP_{PRt}, entopeduncular prereticular nucleus; EPV, ventral entopeduncular nucleus. Other abbreviations: SP, subpopulation

		Basal p3 tegmentum	Alar PHy (associated to cerebral peduncle)					
Gen	**Protein**	**EPA**	**EPV**	**EPD**	**EP_{PRt}**	**EP_{PEm}**	**GPI**	**GPE**
Arx	Aristaless related homeobox							
Chrm3	Cholinergic receptor, muscarinic 3, cardiac							
Foxp2	Forkhead box P2						SP	
Pvalb	Parvalbumin, PV						SP	SP
Trpc4	TRCP4 receptor						SP	SP
Gad1 (Gad67)	Glutamic acid decarboxylase 67 (GAD67)							
Cbln2	Cerebellin 2 precursor protein	SP	SP				SP	
Nkx2.1	NK2 homeobox 1	SP						
Slc32a1	Vesicular GABA transporte (vGAT)	SP					?	
Spp1	Secreted phosphoprotein 1		SP					SP
Rgs4	Regulator of G-protein signaling 4		SP					
Meis1	Meis homeobox 1		SP					
Barhl2	BarH-like 2 (Drosophila)			SP				
Cacna2d1	Calcium channel, voltage-dependent, alpha2/delta subunit 1			SP				
		Basal p3 tegmentum	**Alar PHy (associated to cerebral peduncle)**					**Basal p3 tegmentum**
Gen	**Protein**	**EPA**	**EPV**	**EPD**	**EP_{PRt}**	**EP_{PEm}**	**GPI**	**GPE**
Calb1	Calbindin (CB)			SP			SP	
Crtac1	Cartilage acidic protein 1							
Cyp26b1	Cytochrome P450, family 26, subfamily b, polypeptide 1							
Gabra5	Gamma-aminobutyric acid (GABA) A receptor, subunit alpha 5							
Gabrg1	Gamma-aminobutyric acid (GABA) A receptor, subunit gamma 1			SP				

		Basal p3 tegmentum	Alar PHy (associated to cerebral peduncle)					
Gen	**Protein**	**EPA**	**EPV**	**EPD**	**EP_{PRt}**	**EP_{PEm}**	**GPI**	**GPE**
Nos1	Nitric oxide synthase 1, neuronal			SP				
Pax6	Paired box 6 (PAX6)							
Pbx3	Pre-B cell leukemia Hobeobox 3			migrated cells from PThE?				
Plcl1	Phospholipase C-like 1							
Pou2f2	POU domain, class 2, transcription factor 2							
Slc17a6 (vGlut2)	Solute carrier family 17 (sodium-dependent inorganic phosphate cotransporter), member 6 (vGlut2)							
Synpr	Synaptoporin			SP				
Sst	Somatostatin (SST)			SP				
Stxbp6	Syntaxin binding protein 6 (amisyn)			SP				SP
		Basal p3 tegmentum	**Alar PHy (associated to cerebral peduncle)**					**Basal p3 tegmentum**
Gen	**Protein**	**EPA**	**EPV**	**EPD**	**EP_{PRt}**	**EP_{PEm}**	**GPI**	**GPE**
Tbr1	T-box brain gene 1							
Zfhx3	Zinc Finger Homeobox 3							
Nr2f1 (Tf1)	Nuclear receptor subfamily 2, group F, member 1							
Cacna2d3	Calcium channel, voltage-dependent, alpha2/delta subunit 3							
Cdh6	Cadherin 6				SP			
Ecel1	Endothelin converting enzyme-like 1							
Isl1	ISL1 transcription factor, LIM/homeodomain							
Meis2	Meis homeobox 2							SP
Enc1	Ectodermal-neural cortex 1				SP			SP
Esrrg	Estrogen-related receptor gamma				SP			
Kitl	Kit ligand				SP			
Six3	Sine oculis-related homeobox 3				SP			
Foxg1	Forkhead Box G1							
Chat	Choline acetyltransferase							
Nr4a2	Nuclear receptor subfamily 4, group A, member 2						SP	
Nxph4	Neurexophilin 4						SP	

		Basal p3 tegmentum	Alar PHy (associated to cerebral peduncle)					
Gen	**Protein**	**EPA**	**EPV**	**EPD**	**EP_{PRt}**	**EP_{PEm}**	**GPI**	**GPE**
Slc18a3	Solute carrier family 18 (vesicular monoamine), member 3							
		Basal p3 tegmentum	**Alar PHy (associated to cerebral peduncle)**					**Basal p3 tegmentum**
Gen	**Protein**	**EPA**	**EPV**	**EPD**	**EP_{PRt}**	**EP_{PEm}**	**GPI**	**GPE**
Etv1	Ets variant 1						???	
Lhx6	LIM homeobox protein 6							
Lhx8	LIM homeobox protein 8							
Oprl1	Opioid receptor-like 1							

Table 4.

Experiments from the Allen Institute for Brain Science with injections into the external globus pallidus (GPE), internal globus pallidus (GPI) or dorsal entopeduncular nucleus (EPD).

Experiment number	Main injection site	Mouse lineage	Tracer	Injection volume (μl)
158373958	GPI	C57BL/6J	EGFP	0.090
647574144	Cholinergic GPI	Ntrk1-IRES-Cre	EGFP	0.055
305024724	EPD	Rbp4-Cre_KL100	EGFP	0.021
511942270	GPE	Pvalb-IRES-Cre	EGFP	0.179
265944167	Cholinergic GPI	Ntrk1-IRES-Cre	EGFP	0.087
300318924	GPI	Htr2a-Cre_KM207	EGFP	0.090
539498984	EPD	Sst-IRES-Cre	EGFP	0.035
278501857	GPI	Htr2a-Cre_KM207	EGFP	0.017

EGFP, enhanced green fluorescent protein.